INTERNATIONAL JOURNAL FOR NUMERICAL AND ANALYTICAL METHODS IN GEOMECHANICS
Int. J. Numer. Anal. Meth. Geomech. (2015)
Published online in Wiley Online Library (wileyonlinelibrary.com). DOI: 10.1002/nag.2482

Constitutive and numerical framework for modeling joints and faults in rock

Howard Schreyer[1]*,† and Deborah Sulsky[1,2]

[1]*Department of Mechanical Engineering, University of New Mexico, Albuquerque, NM, U.S.A.*
[2]*Department of Mathematics and Statistics, University of New Mexico, Albuquerque, NM, U.S.A.*

SUMMARY

A three-dimensional constitutive model for joints is described that incorporates nonlinear elasticity based on volumetric elastic strain, and plasticity for both compaction and shear with emphasis on compaction. The formulation is general in the sense that alternative specific functional forms and evolution equations can be easily incorporated. A corresponding numerical structure based on finite elements is provided so that a joint width can vary from a fraction of an element size to a width that occupies several elements. The latter case is particularly appropriate for modeling a fault, which is considered simply to be a joint with large width. For small joint widths, the requisite equilibrium and kinematic requirements within an element are satisfied numerically. The result is that if the constitutive equation for either the joint or the rock is changed, the numerical framework remains unchanged. A unique aspect of the general formulation is the capability to handle either pre-existing gaps or the formation of gaps. Representative stress–strain plots are given to illustrate both the features of the model and the effects of changes in values of material parameters.

Received 11 June 2015; Revised 23 October 2015; Accepted 4 November 2015

KEY WORDS: joint; fault; nonlinear elasticity; plasticity; constitutive model; numerical implementation

1. INTRODUCTION

This paper describes a basic constitutive equation and numerical algorithm for rock containing either joints or faults. In nature, joints appear roughly as a set of parallel planes with uniform spacing. The width of each joint is typically small. On the other hand, a fault often appears singly and with a width that can be orders of magnitude larger than a joint. Nevertheless, insofar as can be determined, the constitutive features of joints and faults, other than width, are similar. Therefore, in the following, we refer only to joints with the understanding that a fault is simply modeled as a joint with a large width.

The ubiquitous nature of joints in rock mass and its importance in understanding rock mechanics for a variety of applications have been admirably summarized by Cook [1] and Jing [2]. Cook [1] points out two main approaches to understanding the effects of joints. The first approach attempts to describe the aggregate effect of many joints or systems of joints, and the second treats joints as discrete entities. Examples of continuum constitutive models that describe the composite effect of many joints within a representative volume element are given by Murakami *et al.* [3], Cai and Hori [4], Lee [5], Chalhoub and Pouya [6], and Brannon *et al.* [7]. Our approach falls in the second category of a discrete joint model. However, it is hoped that with the efficiencies introduced in our constitutive model and

*Correspondence to: H. Schreyer, Department of Mechanical Engineering, University of New Mexico, Albuquerque, NM, U.S.A.
†E-mail: schreyer@unm.edu

numerical solution, many joints can be studied numerically in order to develop aggregate models suitable for simulations on larger spatial scales.

A difficulty connected with analyzing jointed rock is that there is no way of determining the *in situ* features of either a single joint or a set of joints. Experimental data are often based on joints manufactured in the laboratory [8, 9], and constitutive models for shear are derived frequently on assumed roughness profiles [10, 11]. Trivedi [12] creates joints by fracturing physical specimens, but it is not clear if this is a good replica of a physical joint that contains rubble.

There are numerous instances where modeling is used to fit curves to experimental data. However, focusing on one particular path with a precise matching to experimental data is unwarranted in light of the uncertainty associated with both the properties of *in situ* joints and the variety of stress paths inherent in most problems. The objective of a good constitutive model should be to provide the material response for all paths (Gens *et al.*, [13]). Also, general constitutive models are necessary if a particular path is not known a priori, as in solutions to a general boundary-value problem in which each point can experience a unique path. Our approach is to face the uncertainty of *in situ* joint behavior by formulating and using a constitutive model that reflects the essential characteristics of joints and faults with sufficient flexibility to cover expected responses of joints in a variety of geological settings.

The intent of this study is to present a new joint constitutive model and to combine the realistic but relatively simple model for joints with an efficient numerical solution. Specifically, the numerical formulation allows the joint width to range from a fraction of the mesh size in the discretization of the problem to a width covering several elements. By allowing the joint to have an arbitrary width, faults can be analyzed with the same formulation. The joint and rock follow separate constitutive models. If the joint exists within an element of the mesh, kinematic and equilibrium conditions for the joint and surrounding material (rock) within the element are enforced numerically. The advantage of this approach is that constitutive equations for either the joint or the rock can be modified without changing the computational framework. Furthermore, discontinuities related to a joint can exist within an element.

Because of the significant engineering importance of large-scale failure of earth 'structures' due to shear instability, extensive experimental and micromechanical investigations have been performed on joint behavior under shear. Representative examples of using assumed forms of joint asperities to develop suitable constitutive equations are those of Plesha [10], Haberfield and Johnston [14], Huang *et al.* [15], Seidel and Haberfield [16], Grasselli and Egger [17], and Mihai and Jefferson [18].

There has been much less emphasis placed on joint behavior under normal compaction and extension. However, the experimental work of Bandis *et al.* [19], Desai and Fishman [20], and Saeb and Amadei [21] provide experimental data that show response features in compaction, in addition to data that provide the interaction effect of normal and shear stress in a joint. Of course, behavior under compaction is important even for problems dominated by shear because of the change in normal stress associated with shear-enhanced compaction and dilatation. Wang *et al.* [22] have developed a plasticity model that represents nicely the interactive effects of normal and shear displacements as well as shear anisotropy. However, one of their elasticity parameters depends on total joint compression rather than just the elastic compression, so prediction of unloading is problematic.

The proposed joint model focuses on what we consider to be the essential features of joints including plasticity and nonlinear elasticity under compaction and unloading. The shearing part of the model is nonlinearly elastic up to a limit value of shear that depends on the magnitude of normal stress. Further loading in shear results in plastic softening, dilatation, the reduction of shear stress with joint shear strain, and the transition to Mohr–Coulomb behavior with large shear motion, either monotonic or cyclic. A significant feature of the joint constitutive equation is the capability to handle gaps that are either created or pre-existing through the use of positive plastic normal strain. Such a capability is especially important when waves are transmitted through multiple joints because waves can be trapped between joints when joints open to form gaps. Often, sliding interfaces are introduced to handle joints [23]. In our approach, sliding is handled intrinsically through the constitutive equation. The model is illustrated by examining stress–strain

DOI: 10.1002/nag

response that shows the effects of various material parameters, along with the effects of joint width and gaps.

In the next section, preliminary definitions and the constitutive equation for rock are provided. In the following section, a detailed description of the constitutive equation for joints is given. Then Section 4 provides the details of how rock and joint constitutive features are combined to form composite constitutive features for use in an element-based numerical algorithm. The numerical algorithm is used with a driver program that provides strain or stress paths with results displayed in Section 5 that illustrate features of the joint model with and without a segment of rock. Finally, a summary with conclusions is given in the last section of the paper.

2. PRELIMINARY MATERIAL

2.1. Definitions and notation

A joint can be thought of as a weak plane of rubble between two beds of rock. A photograph illustrating joints in an exposed geological structure is shown as Figure 1. Typically joints appear in sets parallel to the bedding planes of the rock. The spacing between joints within each set may vary from centimeters to 10 m [24]. One set of joints may be offset from a second set by a terminating plane as indicated by the sketch in Figure 2a. It is also possible that a second set of joints may overlay the first where the normal to the joints in one set forms an arbitrary angle with respect to the normal of the second set as indicated in Figure 2b. On the other hand, a fault appears singly, and is not associated with a terminating plane. A joint has not experienced motion in shear whereas a fault has. This feature is illustrated by the offset of a joint set because of a fault in Figure 2c. The width of a joint is considered to be of the order of millimeters to centimeters while the width of a fault may be of the order meters. In the following, the formulation is focused on joints, but the framework of the resulting constitutive equation should be suitable for faults as well.

If a joint is subjected to compression, the fill provides resistance to closure where the normal component of traction is a nonlinear function of the amount of joint closure. A joint is generally considered to provide little or no resistance to tensile stress. The objective is to provide a constitutive equation that provides these features.

Joint constitutive behavior is typically described in terms of the joint plane and its normal. Therefore, components of field variables are expressed relative to a local basis $(\boldsymbol{n},\boldsymbol{t},\boldsymbol{p})$ that is used throughout the paper. A unit vector perpendicular to the plane of the joint is denoted by $\boldsymbol{n}$. If a two-dimensional analysis is considered, a unit vector $\boldsymbol{t}$, tangent to the joint, is added to define the plane.

Figure 1. Photograph of jointed rock.

DOI: 10.1002/nag

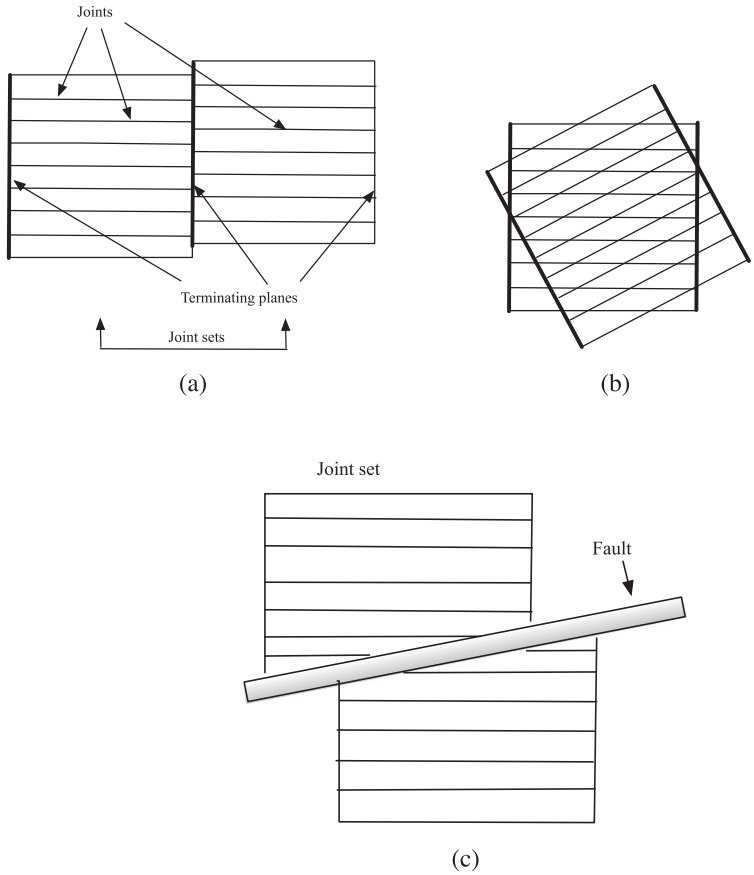

Figure 2. Sketches of joint sets and a fault. (a) One joint set translated with respect to first. (b) One joint set rotated and overlayed with respect to a second joint set. (c) Combination of a joint set and a fault.

For the three-dimensional case followed here, a third unit vector perpendicular to the first two, $\boldsymbol{p} = \boldsymbol{n} \times \boldsymbol{t}$, completes the triad with ***t-p*** lying in the plane of the joint.

Although constitutive equations are constructed independently of numerical techniques, ultimately a numerical procedure must be used to obtain solutions to problems involving wave propagation and material failure. In addition, elastic and plastic strains exist so care must be taken with notation to identify clearly the variables being considered.

Stress, $\boldsymbol{\sigma}$, and strain, $\boldsymbol{e}$, must be determined for the rock, the joint and, later, for an element involving both rock and a joint. A superscript '*R*' is used for the rock, '*J*' for a joint, and no subscript is used for element-based variables. Additional superscripts '*e*' and '*p*' on strain designate elastic and plastic parts, respectively, of the strain tensor. No superscript implies total strain consisting of the sum of elastic and plastic parts. Because the joint material is nonlinear, all constitutive equations will be given in rate form so that the formulation used for numerical implementation is easily obtained with the use of stress and strain increments. A superposed dot represents a derivative with respect to time. Because the formulation is rate independent, any monotonically increasing variable, including time, may be used as a parameter to describe the loading process.

Constitutive equations for rock and joints are considered separately. Then the two are combined within an element using a combination of kinematic and equilibrium constraints. The development of element-based constitutive equations can be carried out either analytically or numerically. The numerical approach is used here so that the overall algorithm is affected only slightly if either the rock or joint constitutive equation is changed. A limitation of our formulation to date is an assumption that the joints are parallel to the sides of square elements.

DOI: 10.1002/nag

2.2. Constitutive equation for rock

It is assumed the rock between joints is isotropic and linearly elastic. The constitutive equation in rate form is

$$\begin{Bmatrix} \dot{\sigma}^R_{nn} \\ \dot{\sigma}^R_{tt} \\ \dot{\sigma}^R_{pp} \end{Bmatrix} = \begin{bmatrix} E^R_1 & E^R_2 & E^R_2 \\ E^R_2 & E^R_1 & E^R_2 \\ E^R_2 & E^R_2 & E^R_1 \end{bmatrix} \begin{Bmatrix} \dot{e}^R_{nn} \\ \dot{e}^R_{tt} \\ \dot{e}^R_{pp} \end{Bmatrix}$$
$$\begin{Bmatrix} \dot{\sigma}^R_{nt} \\ \dot{\sigma}^R_{tp} \\ \dot{\sigma}^R_{pn} \end{Bmatrix} = \begin{bmatrix} 2G^R & 0 & 0 \\ 0 & 2G^R & 0 \\ 0 & 0 & 2G^R \end{bmatrix} \begin{Bmatrix} \dot{e}^R_{nt} \\ \dot{e}^R_{tp} \\ \dot{e}^R_{pn} \end{Bmatrix} \tag{1}$$

in which the elastic constants are

$$E^R_1 = \frac{Y^R(1-v^R)}{(1+v^R)(1-2v^R)} \quad E^R_2 = \frac{v^R}{(1-v^R)}E^R_1 \quad 2G^R = \frac{Y^R}{(1+v^R)} \tag{2}$$

with Y^R denoting Young's modulus, G^R the shear modulus, and v^R Poisson's ratio.

2.3. Generic form for plasticity and related numerical algorithm

The primary focus of this paper is on plasticity as a suitable constitutive model for joints. However, there is no reason why the adjacent rock cannot be modeled also with plasticity. Here, the generic form for plasticity models is summarized together with a simple numerical algorithm used later for numerical simulations. Then the following sections provide various models of elastic-plastic constitutive equations with no need for interspersing details of the numerical approach used for the corresponding constitutive equation subroutine.

For small deformations, the constitutive equation for stress rate in terms of total, $\boldsymbol{e}$, and plastic, $\boldsymbol{e}^P$, strain rates is

$$\dot{\sigma} = \overset{\tan}{\boldsymbol{E}} \cdot\cdot \dot{\boldsymbol{e}}^e \quad \dot{\boldsymbol{e}}^e = \dot{\boldsymbol{e}} - \dot{\boldsymbol{e}}^p \tag{3}$$

in which $\overset{tan}{\boldsymbol{E}}$ denotes the tangent elasticity tensor. Because joints often exhibit nonlinear elasticity, we allow for the possibility that $\overset{tan}{\boldsymbol{E}}$ depends on the elastic strain, $\boldsymbol{e}^e$. Introduce a yield function, F, such that $F<0$ denotes an elastic regime, $F=0$ indicates plastic deformation may be occurring, and $F>0$ is not allowed. Suppose F depends on stress and a set of scalar, history-dependent, effective plastic parameters that are arranged as components of the column vector $\{\bar{e}\}^p$. Introduce a monotonically increasing plasticity parameter, ω, such that evolution equations for the plastic strain tensor and effective plastic strain set are given in rate form as follows:

$$\dot{\boldsymbol{e}}^p = \dot{\omega}\boldsymbol{m} \quad \left\{\dot{\bar{e}}\right\}^p = \dot{\omega}\{m\} \tag{4}$$

in which $\boldsymbol{m}$ is an evolution tensor and each component of $\{m\}$ denotes an evolution function for the corresponding component of $\{\bar{e}\}^p$. The choice of the yield and evolution functions defines the particular plasticity model under consideration. Here, it is assumed that the evolution functions depend on the same variables as the yield function. If an associative flow rule is used, then $\boldsymbol{m} = \partial F/\partial\boldsymbol{\sigma}$.

With the use of (3) and (4), the yield and evolution functions can be implicitly transformed to functions of $\boldsymbol{e}$ and ω. For numerical simulations, we require the term $\partial F/\partial\omega$ with the total strain $\boldsymbol{e}$ fixed. With F assumed to be a function of stress, $\boldsymbol{\sigma}$, and the effective plasticity variables, $\{\bar{e}\}^p$, the rate of F becomes

DOI: 10.1002/nag

$$\dot{F} = \frac{\partial F}{\partial \sigma} \cdot\cdot \dot{\sigma} + \langle \partial F / \partial \langle \overline{e} \rangle^p \rangle \left\{ \dot{\overline{e}} \right\}^p \tag{5}$$

where the bracket <> denotes a row vector. The use of (3) and (4) yields

$$\dot{F} = \frac{\partial F}{\partial \sigma} \cdot\cdot \overset{\tan}{\boldsymbol{E}} \cdot\cdot (\dot{e} - \dot{\omega} \boldsymbol{m}) + \dot{\omega} \langle \partial F / \partial \langle \overline{e} \rangle^p \rangle \{m\} \tag{6}$$

where the last term is the inner product of two vectors. The rate of F becomes

$$\dot{F} = \frac{\partial F}{\partial \boldsymbol{e}} \cdot\cdot \dot{\boldsymbol{e}} + \frac{\partial F}{\partial \omega} \dot{\omega} \tag{7}$$

and (6) is used to obtain

$$\frac{\partial F}{\partial \mathbf{e}} = \frac{\partial F}{\partial \sigma} \cdot\cdot \overset{\tan}{\boldsymbol{E}} \quad \frac{\partial F}{\partial \omega} = -\frac{\partial F}{\partial \sigma} \cdot\cdot \overset{\tan}{\boldsymbol{E}} \cdot\cdot \boldsymbol{m} + \langle \partial F / \partial \langle \overline{e} \rangle^p \rangle \{m\} \tag{8}$$

Theoretically, the consistency condition $\dot{F} = 0$ is used to ensure the yield condition is continually satisfied during plastic deformation. However, a numerical algorithm involves the use of finite increments instead of rates of the strain variables. Typically, increments in total strain are prescribed. Initially, the strain increments are assumed to be elastic, and the yield function is evaluated. When the yield function is positive, the proposed procedure is to force the value of the yield function to 0 while holding the total strain fixed. For this step, F can be considered a function of the scalar variable, ω, so the process is simply one of finding a zero. Because $\partial F/\partial \omega$ is typically available, the Newton–Raphson procedure is appropriate. For simplicity, the values of the functions $\overset{\tan}{\boldsymbol{E}}$, $\partial F/\partial \omega$, $\boldsymbol{m}$ and $\{m\}$ are held fixed, as indicated by a subscript '0', for the iteration procedure used to obtain the solution for the current step. Let ε denote a suitably small positive number. The algorithm is summarized as follows under the assumptions that the increment in total strain $\Delta \boldsymbol{e}$ is prescribed.

Start of Elasto-Plastic Algorithm

1. Update the elasticity tangent tensor $\overset{tan}{\boldsymbol{E}}_0 = \overset{tan}{\boldsymbol{E}}(e^e)$
2. Assume step is elastic. Update total strain, elastic strain and stress:

$$\begin{aligned} &\boldsymbol{e} \leftarrow \boldsymbol{e} + \Delta \boldsymbol{e} \qquad \Delta \boldsymbol{e}^e = \Delta e \\ &\boldsymbol{e}^e \leftarrow \boldsymbol{e}^e + \Delta \boldsymbol{e}^e \quad \boldsymbol{\sigma} \leftarrow \boldsymbol{\sigma} + \overset{tan}{\boldsymbol{E}}_0 \cdot\cdot \Delta \boldsymbol{e}^e \end{aligned} \tag{9}$$

3. Evaluate F.
   (i) If $F \le \varepsilon$, then the step is elastic. A solution has been obtained. Go to Step 9.
   (ii) If $F > \varepsilon$ continue on to Step 4.
4. Evaluate the evolution functions, m_0 and $\{\mathrm{m}\}_0$, and the derivative function, $(\partial \mathrm{F}/\partial \omega)_0$ using the current values of stress, elastic strain, plastic strain and effective plastic strain.

Start of Iteration Loop

5. Obtain an increment in the plasticity parameter:

$$\Delta \omega = -F / (\partial F / \partial \omega)_0$$

6. Obtain increments in plastic and effective plastic strain:

$$\Delta \boldsymbol{e}^p = \Delta \omega \boldsymbol{m}_0 \quad \{\Delta \overline{e}\}^p = \Delta \omega \{m\}_0$$

DOI: 10.1002/nag

7. Update strain and stress variables

$$\boldsymbol{e}^p \leftarrow \boldsymbol{e}^p + \Delta\boldsymbol{e}^p \qquad \{\overline{e}\}^p \leftarrow \{\overline{e}\}^p + \Delta\{\overline{e}\}^p$$
$$\Delta\boldsymbol{e}^e = -\Delta\boldsymbol{e}^p \qquad \boldsymbol{e}^e \leftarrow \boldsymbol{e}^e + \Delta\boldsymbol{e}^e$$
$$\boldsymbol{\sigma} \leftarrow \boldsymbol{\sigma} + \overset{\tan}{\boldsymbol{E}}_0 \cdot\cdot \Delta\boldsymbol{e}^e$$

8. Evaluate F. If $F \leq \varepsilon$, go to Step 9; otherwise go to Step 5.

End of Iteration Loop

9. Exit the algorithm.

End of Elasto-Plastic Algorithm

Higher-order algorithms can be obtained by evaluating $\boldsymbol{m}$, $\{m\}$, $\partial F/\partial\omega$, and $\overset{\tan}{\boldsymbol{E}}$ within the iterative loop. However, strain increments are often small enough that this added expense is not necessary.

3. CONSTITUTIVE EQUATIONS FOR JOINTS

3.1. Joint strains

The width of the joint is denoted as w^J. Let z be the normal coordinate with respect to the mid-plane of a point in the direction $\boldsymbol{n}$ as indicated in Figure 3. If $\boldsymbol{u}$ denotes the displacement of a material point within the joint, then the relative displacement components for corresponding points at the upper and lower surfaces of the joint are defined to be

$$\widehat{\boldsymbol{u}} = \widehat{u}_n\boldsymbol{n} + \widehat{u}_t\boldsymbol{t} + \widehat{u}_p\boldsymbol{p} = \boldsymbol{u}\big|_{z=w^J/2} - \boldsymbol{u}\big|_{z=-w^J/2} \tag{10}$$

The displacement field within the joint is assumed to be linear in z. The result is that $\hat{u}_n$ is the net opening of the joint. Many authors choose the net closure to be positive, and for uniaxial strain, the net closure is the volumetric compaction. Similarly $\hat{u}_t$ and $\hat{u}_p$ denote the relative tangential displacement components of the joint surfaces. Here, we use a sign convention, and components of

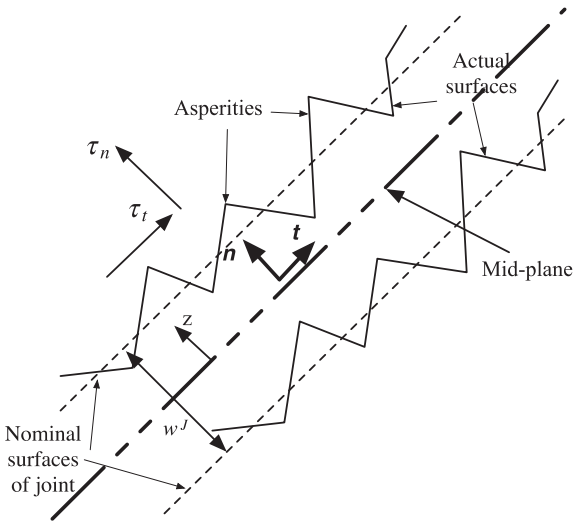

Figure 3. Notation for a joint.

DOI: 10.1002/nag

strain rather than relative surface displacements, to describe the kinematic behavior of the joint so that the usual three-dimensional notation of continuum mechanics can be used. The normal and transverse shear components of joint strain are defined to be

$$e^J_{nn} = \frac{\widehat{u}_n}{w^J} \quad e^J_{nt} = \frac{\widehat{u}_t}{2w^J} \quad e^J_{pn} = \frac{\widehat{u}_p}{2w^J} \tag{11}$$

with the assumption that $w^J \neq 0$. A joint with 0 width can be treated within a constitutive framework as a sliding interface if the normal component of stress is negative and allowed to open into a gap with zero traction if the kinematics of the problem requires such a state.

The remaining components of joint strain $\left\{e^J_{tt}, e^J_{pp}, e^J_{tp}\right\}$ are assumed to be based on the usual small-deformation continuum approach and are of much less significance for our purposes than the components defined in (11).

It is assumed that the joint strain is a linear combination of elastic and plastic parts

$$\boldsymbol{e}^J = \boldsymbol{e}^{J,e} + \boldsymbol{e}^{J,p} \tag{12}$$

and that the plastic parts of the strain components $\left\{\boldsymbol{e}^J_{tt}, \boldsymbol{e}^J_{pp}, \boldsymbol{e}^J_{tp}\right\}$ are 0.

3.2. Joint elasticity

Experimental data for joints typically exhibit both nonlinearly elastic and plastic behavior. A sketch of typical features of experimental data for compaction is given in Figure 4.

If the elastic part is assumed to be isotropic, the elastic constitutive equation in rate form is chosen to be analogous to (1) as follows:

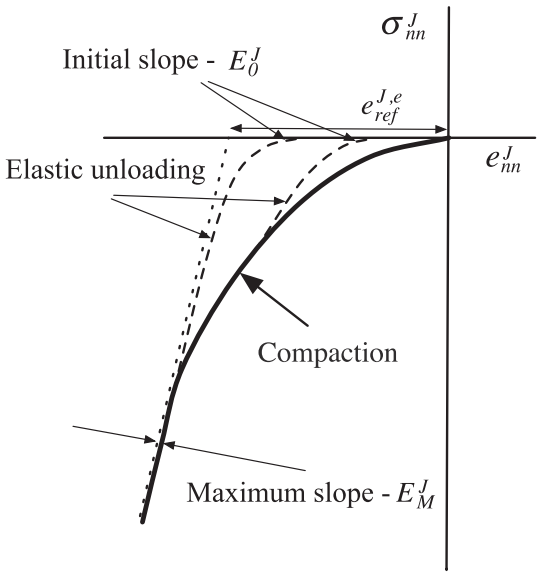

Figure 4. Observed features for normal compaction and unloading of a joint.

DOI: 10.1002/nag

$$\begin{Bmatrix} \dot{\sigma}^J_{nn} \\ \dot{\sigma}^J_{tt} \\ \dot{\sigma}^J_{pp} \end{Bmatrix} = \begin{bmatrix} \overset{\tan}{E}{}^J_1 & \overset{\tan}{E}{}^J_2 & \overset{\tan}{E}{}^J_2 \\ \overset{\tan}{E}{}^J_2 & \overset{\tan}{E}{}^J_1 & \overset{\tan}{E}{}^J_2 \\ \overset{\tan}{E}{}^J_2 & \overset{\tan}{E}{}^J_2 & \overset{\tan}{E}{}^J_1 \end{bmatrix} \begin{Bmatrix} \dot{e}^{J,e}_{nn} \\ \dot{e}^{J,e}_{tt} \\ \dot{e}^{J,e}_{pp} \end{Bmatrix}$$
$$\begin{Bmatrix} \dot{\sigma}^J_{nt} \\ \dot{\sigma}^J_{tp} \\ \dot{\sigma}^J_{pn} \end{Bmatrix} = \begin{bmatrix} \overset{\tan}{2G}{}^J & 0 & 0 \\ 0 & \overset{\tan}{2G}{}^J & 0 \\ 0 & 0 & \overset{\tan}{2G}{}^J \end{bmatrix} \begin{Bmatrix} \dot{e}^{J,e}_{nt} \\ \dot{e}^{J,e}_{tp} \\ \dot{e}^{J,e}_{pn} \end{Bmatrix} \tag{13}$$

in which the superscript 'J' indicates these terms are applicable to the joint, and the over-script 'tan' emphasizes the point that these are the elastic tangent parameters. The following assumptions are invoked: (i) Poisson's ratio for the joint is the constant v^J_0; and (ii) the other independent modulus is a function of the elastic volumetric strain, $e^{J,e}_{vol}$.

Obtaining experimental values for Poisson's ratio for joints is difficult, and the assumption of a constant value is rather extreme. However, solutions for stress are often not overly sensitive to values of Poisson's ratio, especially in light of the large variations in values of other constitutive parameters. An assumed value of $v^J_0 = 0.2$ is considered reasonable. To obtain an expression for the tangent modulus E^J_1, suppose that experimental compaction data are available for uniaxial strain with e^J_{nn}, the only nonzero component of strain. The elastic part, $e^{J,e}_{nn}$, is obtained by unloading. For this loading path, the volumetric strain equals the only nonzero component of strain, or

$$e^{J,e}_{vol} = e^{J,e}_{nn} \tag{14}$$

Presumably, σ^J_{nn} is measured so that the relationship

$$\sigma^J_{nn} = g^e\left(e^{J,e}_{vol}\right) \tag{15}$$

is available from experimental data. Also, for uniaxial strain

$$\dot{\sigma}^J_{nn} = \overset{\tan}{E}{}^J_1 \dot{e}^{J,e}_{nn} \tag{16}$$

so that the tangent modulus, again based on experimental data, is

$$\overset{\tan}{E}{}^J_1 = \frac{\partial g^e}{\partial e^{J,e}_{nn}} \equiv f^e\left(e^{J,e}_{vol}\right) \tag{17}$$

The other tangent moduli become

$$\overset{\tan}{E}{}^J_2 = \frac{v^J_0}{\left(1 - v^J_0\right)} \overset{\tan}{E}{}^J_1 \quad \overset{\tan}{2G}{}^J = \frac{\left(1 - 2v^J_0\right)}{\left(1 - v^J_0\right)} \overset{\tan}{E}{}^J_1 \tag{18}$$

If desired, the tangent Young's and bulk moduli are

$$\overset{\tan}{Y}{}^J = \overset{\tan}{E}{}^J_1 \frac{\left(1 + v^J_0\right)\left(1 - 2v^J_0\right)}{\left(1 - v^J_0\right)} \qquad \overset{\tan}{B}{}^J = \overset{\tan}{E}{}^J_1 \frac{\left(1 + v^J_0\right)}{3\left(1 - v^J_0\right)} \tag{19}$$

DOI: 10.1002/nag

For explicit numerical analyses, it is convenient to use an analytical form for the elastic function, g^e, with a small number of material parameters obtained using a best fit to experimental data. A proposed form and its derivative are considered under a number of simplifying but plausible assumptions given as follows:

1. If the elastic volumetric strain is positive, it is assumed the joint cannot sustain stress so the elastic function must then be 0,
2. For small elastic volumetric strain, $\overset{\tan}{E}{}_1^J = E_0^J$, a constant with small value,
3. As the elastic volumetric strain increases negatively from 0, the modulus $\overset{\tan}{E}{}_1^J$ increases from E_O^J to a maximum large, constant value of E_M^J at a reference, elastic, volumetric, negative strain of a constant $e_{ref}^{J,e}$,
4. For $e_{vol}^{J,e} \le e_{ref}^{J,e}$, the tangent modulus $\overset{\tan}{E}{}_1^J$ remains fixed at the maximum value E_M^J, and
5. Because the rubble in the joint is based on the surrounding rock, the maximum value of the tangent modulus equals the corresponding value of the tangent modulus of rock, or

$$E_M^J = E_1^R \tag{20}$$

The proposed forms for the elastic function and its derivative are

$$\begin{aligned}
g^e\left(e_{vol}^{J,e}\right) &= 0 && e_{vol}^{J,e} > 0 \\
g^e\left(e_{vol}^{J,e}\right) &= E_0^J\, e_{vol}^{J,e} + \left(E_M^J - E_0^J\right)\frac{e_{ref}^{J,e}}{m^e}\left\{\frac{e_{vol}^{J,e}}{e_{ref}^{J,e}}\right\}^{m^e} && e_{ref}^{J,e} \le e_{vol}^{J,e} \le 0 \\
g^e\left(e_{vol}^{J,e}\right) &= g_{tr}^e + E_M^J\left(e_{vol}^{J,e} - e_{ref}^{J,e}\right) && e_{vol}^{J,e} < e_{ref}^{J,e}
\end{aligned} \tag{21}$$

and

$$\begin{aligned}
\overset{\tan}{E}{}_1^J &= 0 && e_{vol}^{J,e} > 0 \\
\overset{\tan}{E}{}_1^J &= E_0^J + \left(E_M^J - E_0^J\right)\left\{\frac{e_{vol}^{J,e}}{e_{ref}^{J,e}}\right\}^{m^e-1} && \mathrm{e}_{ref}^{J,e} \le e_{vol}^{J,e} \le 0 \\
\overset{\tan}{E}{}_1^J &= E_M^J && e_{vol}^{J,e} < \mathrm{e}_{ref}^{J,e}
\end{aligned} \tag{22}$$

respectively. Note that $e_{ref}^{J,e}$ is negative and the stress, g_{tr}^e, at which g^e transitions to a linear function is the value when $e_{vol}^{J,e} = e_{ref}^{J,e}$, or

$$g_{tr}^e = \left[E_0^J + \frac{E_M^J - E_0^J}{m^e}\right] e_{ref}^{J,e} \tag{23}$$

With E_M^J given by (20), the remaining material parameters that must be assigned values are E_0^J, v_0^J, $e_{ref}^{J,e}$, and m^e of which the latter is dimensionless. Presumably, values for these parameters can be obtained by obtaining a best fit to experimental data.

3.3. Joint plasticity

3.3.1. Assumptions. The formulation for joint plasticity is constructed to obtain the following perceived features as exhibited by experimental data:

DOI: 10.1002/nag

1. Under compaction (uniaxial strain), the initial response is much softer than elasticity as exhibited by unloading. Therefore, plasticity must occur immediately and with increased compaction, the ratio of plastic to elastic strain rate continually decreases until the joint behaves as a linear elastic material under large pressure.
2. The joint exhibits no strength in tension.
3. The shear strain (due to tangential motion) may be several orders of magnitude larger than the normal components of strain.
4. After sufficiently large shear motion, continued response in shear is governed by Coulomb's friction criterion.
5. Even with no compressive component of traction, joints exhibit resistance to shear because of the surface roughness in the form of asperities between the mating surfaces.
6. After a certain amount of shear, the asperities wear down and any accompanying cohesive strength in shear is lost.
7. Compressive traction enhances the apparent strength in shear because of asperities, and
8. Asperities cause dilatation under shear.

These are the features incorporated into the model outlined next.

3.3.2. Basic structure. A conventional plasticity model requires a yield surface and evolution equations for plastic strains and other internal plasticity variables. A particular model requires specific forms for a yield function and the evolution functions.

To emphasize the various aspects of plasticity, normal and shear components of traction within the joint are introduced as follows:

$$\tau_n^J = \sigma_{nn}^J \quad \tau_t^J = \sigma_{nt}^J \quad \tau_p^J = \sigma_{pn}^J \tag{24}$$

A classical approach for continuum plasticity is to assume a yield function depends on pressure and shear. For joints, experimental data are generally available for only two categories of tests, namely, compaction under uniaxial strain and shear under specified normal traction. In other words, only the components of stress identified in (24) are considered. Here, yield functions are developed based on these components. However, the model is intended for three-dimensional applications in which case there is the implicit assumption that the effect of the remaining components of stress, $\sigma_{pp}^J, \sigma_{tt}^J$, and σ_{tp}^J, are insignificant as far as plasticity is concerned.

Define an effective shear stress for the joint to be

$$\tau_s^J = \left[\tau_t^{J2} + \tau_p^{J2}\right]^{1/2} \tag{25}$$

A yield function for the joint, F^J, is assumed to depend on τ_n^J and τ_s^J with the usual criteria that $F_J < 0$ indicates elastic behavior, yielding occurs if $F^J = 0$, and $F^J > 0$ is not allowed theoretically. The yield surface $F^J = 0$ is taken to be a combination of three individual yield surfaces for compaction, effective shear, and tension:

$$F_C = 0 \quad F_S = 0 \quad F_T = 0 \tag{26}$$

Expressed alternatively, the value of the joint yield function is the maximum of values for these yield functions, or

$$F^J = \max(F_C, F_S, F_T) \tag{27}$$

The proposed forms for the yield surfaces described by (26) and (27) with and without asperities are illustrated in Figure 5.

Next, a detailed description for each individual yield surface is given.

DOI: 10.1002/nag

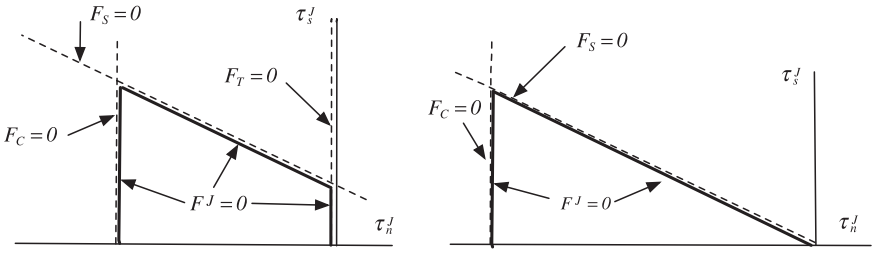

Figure 5. Yield surface for joint in space of traction components. (a) Yield surface with asperities. (b) Yield surface without asperities.

3.3.3. Compaction. For compaction, it is assumed that the dominant effect is captured through the use of normal components of stress, τ_n^J, and plastic strain, $e_{nn}^{J,p}$. This simple structure does not include coupling with shear through shear-enhanced compaction. The yield function for compaction only is assumed to be

$$F_C = \tau_{cy}^J - \tau_n^J \tag{28}$$

where the yield stress in compaction, τ_{cy}^J, is chosen to be negative for negative values of $e_{nn}^{J,p}$. Therefore, $F_C < 0$ (elastic) if $\tau_n^J > \tau_{cy}^J$. The yield function is assumed to be 0 for positive plastic strain. A feature consistent with that of elastic behavior for large compaction is obtained by choosing the yield stress to become negatively infinite as $e_{nn}^{J,p} \to e_0^{J,p}$, where $e_0^{J,p}$ is a negative material constant. One possible form is the following:

$$\begin{aligned} \tau_{cy}^J &= E_0^{J,p} = \frac{e_0^{J,p}}{m^p}\left[\left\{\frac{e_0^{J,p}}{e_0^{J,p} - e_{nn}^{J,p}}\right\}^{m^p} - 1\right] \quad && e_{nn}^{J,p} \le 0 \\ \tau_{cy}^J &= 0 && e_{nn}^{J,p} > 0 \end{aligned} \tag{29}$$

in which the value 0 for τ_{cy}^J has been imposed for zero plastic strain because experimental data indicate a very small value for the initial yield stress. Additional material parameters are E_{J0}^p and m^p of which the latter is dimensionless. The tangent plastic modulus is defined to be

$$\overset{\tan}{E}{}^{J,p} = \frac{\partial \tau_{cy}^J}{\partial e_{Jnn}^p} = E_0^{J,p}\left\{\frac{e_0^{J,p}}{e_0^{J,p} - e_{nn}^{J,p}}\right\}^{m^p - 1} \tag{30}$$

so that E_{J0}^p can be interpreted as the plastic modulus for zero plastic strain.

Suppose unloading occurs from a compacted state so that the normal component of traction is increasing. This phase of the response is purely elastic until the stress reduces to 0. If the unloading continues as specified by further positive increments in joint opening, then the elastic joint strain remains 0, but the plastic strain, which now equals the total strain, is allowed to increase with a corresponding reduction in absolute value of yield stress. With even more unloading, the joint plastic strain is positive and a gap forms of magnitude $e_{nn}^{J,p} w^J$. Then if the loading process is reversed, the gap closes, and upon further compaction, the original stress–strain curve is recovered. If experimental data indicate that cyclic loading causes a change in the stress–strain curve, then a kinematic feature must be incorporated into the formulation.

For compaction, the evolution equation for plastic strain is assumed to be based on an associated flow rule, or

DOI: 10.1002/nag

$$\dot{e}_{nn}^{J,p} = \dot{\omega}_c \frac{\partial F_C}{\partial \tau_n^J} = -\dot{\omega}_c \tag{31}$$

The use of (31) and (8) yields

$$\frac{\partial F}{\partial \omega_c} = -\left(\overset{\tan}{E}{}_1^J + \overset{\tan}{E}{}^{J,p} \right) \tag{32}$$

which is the conventional form used in the Newton–Raphson procedure to find an increment $\Delta\omega_c$.

Because of the exponential forms used for both the elasticity and the yield function, convergence may be extremely slow. With numerical experimentation, an approximate form of $\partial F/\partial\omega_c$ is used to reduce the number of iterations. A form that has appeared to be robust is

$$\left.\frac{\partial F}{\partial \omega_c}\right|_{approx} = -\left(\overset{\tan}{E}{}_1^J + 10\overset{\tan}{E}{}^{J,p} \right) \tag{33}$$

The iterations are terminated when

$$\frac{F}{1 + \left|\tau_{cy}^J\right| + \left|\tau_n^J\right|} \leq 0.005 \tag{34}$$

Recall that the other two normal components of plastic strain rate are assumed to be 0. Because both the normal components of traction and of rate of plastic strain are always negative, plastic compaction results in positive dissipation.

In summary, an outline has been given for describing the response of a joint to compaction. The plastic material parameters that must be specified are $\left\{e_0^{J,p}, E_{J0}^p, m^p\right\}$.

If the yield condition indicates that loading is elastic in the compressive regime, then the total strain components equal the elastic strain components, and the constitutive equation reduces to

$$\dot{\tau}_n^J = \overset{\tan}{E}{}_1^J \dot{e}_{nn}^{J,e} + \overset{\tan}{E}{}_2^J \left(\dot{e}_{tt}^{J,e} + \dot{e}_{pp}^{J,e} \right) \tag{35}$$

where the elastic tangent components must be evaluated for the current value of elastic volumetric strain.

3.3.4. Shear. Consider the case where the normal component of traction is negative or 0. If τ_s^J denotes the effective shear defined in (25) and τ_{sy}^J represents the yield stress in shear, then the corresponding yield function for shear is chosen to be

$$F_S = \tau_s^J - \tau_{sy}^J \tag{36}$$

Note that $\tau_s^J \geq 0$, so the additional restriction is imposed that $\tau_{sy}^J \geq 0$. Then $F_S \geq 0$ if $\tau_s^J \geq \tau_{sy}^J$.

There is assumed to be some inherent resistance in shear, or cohesion τ_{as}^J, because of the asperities of opposing surfaces. After these asperities are worn off, it is assumed further that the tangential motion is governed by the Mohr–Coulomb criterion. To reflect these features, the yield stress in shear is assumed to be

$$\tau_{sy}^J = \tau_{as}^J - \mu^J \tau_n^J \tag{37}$$

in which μ^J is a material constant, the friction coefficient for material in the joint. Recall that τ_n^J is negative. Barton [25] argues persuasively that the linear relation involving τ_n^J is not accurate when

DOI: 10.1002/nag

the absolute value of τ_n^J is large, and that a limiting value for shear failure is reached. To accommodate this feature, a nonlinear function of τ_n^J should be used in (37).

Next, we define a measure of the inelastic motion in shear. Effective plastic strain for shear is defined to be

$$\widehat{e}_s^{J,p} = \int \dot{\widehat{e}}_s^{J,p} dt \qquad \dot{\widehat{e}}_s^{J,p} = \left\{ \left(\dot{e}_{nt}^{J,p}\right)^2 + \left(\dot{e}_{pn}^{J,p}\right)^2 \right\}^{1/2} \tag{38}$$

For any given problem consisting of cyclic tangential motion, it is quite possible that $\widehat{e}_s^{J,p} \gg 1$ even if the relative tangential displacement of the joint surfaces is small.

The cohesion is assumed to decay monotonically with an increase in the effective inelastic shear displacement. For simplicity, a linear relation is assumed:

$$\tau_{as}^J = \tau_{a0}^J R_a \left[1 - \frac{\widehat{e}_s^{J,p}}{e_{a0}^{J,p}} \right] \tag{39}$$

in which τ_{a0}^J denotes the initial shear strength because of asperities. The ramp function is defined to be $R_a[\alpha] = \alpha$ if $\alpha \geq 0$ and $R_a[\alpha] = 0$ if $\alpha < 0$. Therefore, $e_{a0}^{J,p}$ is the effective plastic shear strain at which the strength due to asperities is lost, and the cohesive strength due to asperities remains 0 for $\widehat{e}_s^{J,p} > e_{s0}^{J,p}$.

Suppose an associated flow rule is used to obtain evolution equations for the plastic components of shear strain, $e_{nt}^{J,p}$, $e_{np}^{J,p}$, and normal plastic joint strain, $e_{nn}^{J,p}$, so that

$$\begin{aligned} \dot{e}_{nt}^{J,p} &= \dot{\omega}_s \frac{\partial F_S}{\partial \tau_t^J} = \dot{\omega}_s \frac{\tau_t^J}{\tau_s^J} \\ \dot{e}_{np}^{J,p} &= \dot{\omega}_s \frac{\partial F_S}{\partial \tau_p^J} = \dot{\omega}_s \frac{\tau_p^J}{\tau_s^J} \\ \dot{e}_{nn}^{J,p} &= \dot{\omega}_s \frac{\partial F_S}{\partial \tau_n^J} = \mu^J \dot{\omega}_s \end{aligned} \tag{40}$$

in which ω_s is a monotonically increasing plasticity parameter and the following equation has been used for the derivative with respect to τ_t^J:

$$\frac{\partial F_S}{\partial \tau_t^J} = \frac{\partial F_S}{\partial \tau_s^J} \frac{\partial \tau_s^J}{\partial \tau_t^J} = \frac{\tau_t^J}{\tau_s^J} \tag{41}$$

with a corresponding relation for the other component of shear. It follows from (25) and (38) that

$$\dot{\widehat{e}}_s^{J,p} = \dot{\omega}_s \frac{\partial F_S}{\partial \tau_s^J} = \dot{\omega}_s \tag{42}$$

Note that $\dot{\widehat{e}}_{nn}^{J,p}$ is always positive that indicates that plastic dilatation is occurring under shear motion. With dilatation, the current yield strength for compaction is reduced and represents a coupling effect between shear and normal motion. This is a result expected because of the effect of asperities and is included in the combined model.

Once the asperities have worn off, it is assumed that the result is simple Mohr–Coulomb friction, in which case no more dilatation is expected. To reflect the pure-slip case after the asperities are eliminated, a non-associated flow rule is proposed instead of the associated flow rule so that the rate of the normal component of plastic strain transitions to 0 with shear deformation. To provide a smooth transition from dilatation to zero normal component, the last evolution equation of (40) is replaced with

DOI: 10.1002/nag

$$\dot{e}_{nn}^{J,p} = \dot{\omega}_s \frac{\partial F_S}{\partial \tau_n^J} R_a \left[1 - \frac{e_s^{J,p}}{e_{a0}^{J,p}}\right] = \dot{\omega}_s \, \mu^J R_a \left[1 - \frac{e_s^{J,p}}{e_{a0}^{J,p}}\right] \tag{43}$$

The implication is that the evolution equation is non-associative for both regimes of asperity decay and Mohr–Coulomb friction.

Using the elastic constitutive relations of (13), the definition of (39), and the plasticity evolution equations of (42) and (43), it follows from (8) that

$$\frac{\partial F}{\partial \omega_s} = -2\overset{\tan}{G}{}^J - \overset{\tan}{E}{}_1^J \left(\mu^J\right)^2 R_a \left[1 - \frac{e_s^{J,p}}{e_{a0}^{J,p}}\right] + \frac{\tau_{a0}^J}{e_{a0}^{J,p}} H_e \left[1 - \frac{e_s^{J,p}}{e_{a0}^{J,p}}\right] \tag{44}$$

in which $H_e[]$ denotes the Heaviside function. To ensure that the yield function reduces monotonically in the Newton–Raphson procedure, care must be taken in the selection of material parameters so that $\partial F/\partial \omega_s$ is always negative. Because the positive part of $\partial F/\partial \omega_s$ in (44) is due to softening, a positive value of $\partial F/\partial \omega_s$ is a definition of material instability. To ensure stability, the material parameters must satisfy

$$2\overset{\tan}{G}{}^J + \overset{\tan}{E}{}_1^J \left(\mu^J\right)^2 - \frac{\tau_{a0}^J}{e_{a0}^{J,p}} \geq 0 \quad \text{(stability)} \tag{45}$$

If a finite element contains both joint and rock, then the softening feature is magnified by elastic unloading in the rock. Therefore for numerical simulations, condition (45) is a necessary but not a sufficient condition for stability of the element constitutive equation.

During the softening regime, the asperities cause dilatation, $\dot{e}_{nn}^{J,p} > 0$, and this will have the effect of changing the location of the yield surface for compaction. After the effect of asperities has been erased, (44) reduces to $\partial F/\partial \omega_s = 2\overset{\tan}{G}{}^J$, and the shear yield condition is one of perfect plasticity with a non-associated flow law that yields $\dot{e}_{nn}^{J,p} = 0$ and is consistent with the Mohr–Coulomb criterion.

3.3.5. Tensile state. If $\tau_n^J = 0$, it is assumed the joint offers no resistance to motion in either the normal or tangential directions. Positive values for τ_n^J are not allowed to exist. This case is handled by defining a yield function, F_T, for the tensile state as follows:

$$F_T = \tau_{Jn} \tag{46}$$

With the assumption that the components of shear $\left(\tau_t^J, \tau_p^J\right)$ must also be 0 when the normal component of traction is 0, the evolution equations for plastic strain are chosen simply to maintain zero rates for these stress components. Recall that for increments in strain, the relevant elastic constitutive equations are

$$\begin{aligned}
\Delta\tau_n^J &= \overset{\tan}{E}{}_1^J \left(\Delta e_{nn}^J - \Delta e_{nn}^{J,p}\right) + \overset{\tan}{E}{}_2^J \left(\Delta e_{tt}^J + \Delta e_{pp}^J\right) \\
\Delta\tau_t^p &= 2\overset{\tan}{G}{}^J \left(\Delta e_{np}^J - \Delta e_{np}^{J,p}\right) \\
\Delta\tau_p^J &= 2\overset{\tan}{G}{}^J \left(\Delta e_{np}^J - \Delta e_{np}^{J,p}\right)
\end{aligned} \tag{47}$$

with the total strain increments prescribed. The solutions for the increments in plastic strain that yield zero increments in components of traction are

DOI: 10.1002/nag

$$\Delta e_{nn}^{J,p} = \Delta e_{nn}^{J} + \frac{v_0^J}{\left(1 - v_0^J\right)}\left(\Delta e_{tt}^{J} + \Delta e_{pp}^{J}\right) \quad \Delta e_{nt}^{J,p} = \Delta e_{nt}^{J} \quad \Delta e_{np}^{J,p} = \Delta e_{np}^{J} \tag{48}$$

in which (18) has been used for the term involving Poisson's ratio. However, it is assumed that when the normal stress is 0, shear motion does not contribute to the decay of asperities so that (42) is replaced with $\Delta \widehat{e}_s^{\,J,p} = 0$. The result is that the appearance of joint opening and relative sliding is handled as a constitutive equation and reflected through the normal and shear components of joint plastic strain. This precludes the need for an alternative approach such as a slide-line algorithm.

Recall that the plasticity contributions of the remaining strain components are assumed to be insignificant, or the elastic strain increments equal the total strain increments. Therefore, the equations for the other increments of stress become the plane-stress relations

$$\begin{aligned}
\Delta\sigma_{tt}^{J} &= \frac{\left(1 - 2v_0^J\right)}{\left(1 - v_0^J\right)^2} \overset{\tan}{E}{}_1^J \left[\Delta e_{tt}^{J} + v_0^J \Delta e_{pp}^{J}\right] \\
\Delta\sigma_{pp}^{J} &= \frac{\left(1 - 2v_0^J\right)}{\left(1 - v_0^J\right)^2} \overset{\tan}{E}{}_1^J \left[\Delta e_{pp}^{J} + v_0^J \Delta e_{tt}^{J}\right] \\
\Delta\sigma_{tp}^{J} &= 2\overset{\tan}{G}{}^J \Delta e_{tp}^{J}
\end{aligned} \tag{49}$$

3.3.6. Summary of composite yield function. With the three yield functions defined previously, the composite yield function, F^J, is defined to be

$$F^J = \max(F_C, F_S, F_T) \tag{50}$$

where

$$F_C = \tau_{ny}^J - \tau_n^J \quad F_S = \tau_s^J - \tau_{sy}^J \quad F_T = \tau_n^J \tag{51}$$

The composite yield surface is given simply by $F^J = 0$.

To illustrate how the composite yield surface behaves under a couple of paths, sketches are provided in Figure 6. Because the initial yield stress is very small, the surfaces $F_C = 0$ and $F_T = 0$ are nearly coincident as indicated in Figure 6(a). With loading in compaction, with or without some shear as suggested by the paths (i) and (ii) shown in Figure 6(b), the surface $F_C = 0$ moves to the left with the other segments of the surface stationary.

Next, consider the path identified as 0-(i)-(ii)-(iii) with '0' denoting the origin as shown in Figure 6(c). First the compaction yield surface is pushed out to configuration (a). Then for the next segment of loading, the normal component of traction is reduced, but the shear part is increased so that the shear yield surface, designated (c), is reached. Shear softening occurs because of ablation of asperities. While softening, dilatation is occurring that causes the compaction surface to move inward to location (b). The yield surface decays until the Mohr–Coulomb surface, designated as (d), is reached after which the yield surface in shear remains stationary. When unloading, the three components of traction satisfy the elastic relation.

There is the possibility that the revised location of the compaction yield surface will cause both yield surfaces to be simultaneously activated. The approach proposed here is to simply apply the yield conditions one at a time until both are satisfied. A mathematically rigorous approach is to satisfy both criteria simultaneously.

Once the effect of asperities is gone, it is assumed that cohesion is lost; there is no further dilatation, and the shear surface is associated with sliding only.

DOI: 10.1002/nag

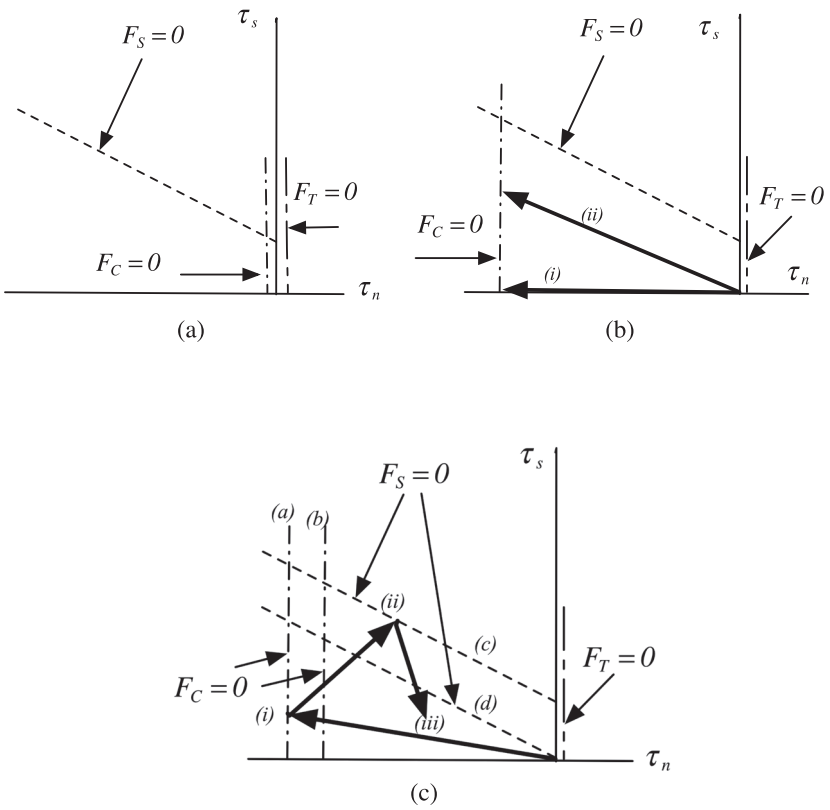

Figure 6. Evolution of yield surfaces in space of traction components. (a) Initial location of surfaces. (b) Location of yield surfaces with compaction involving (i) no shear and (ii) a small amount of shear. (c) Yield surfaces after a complex path involving compaction and shear.

In summary, after some compaction with small or no shear, the composite yield surface appears as shown in Figure 5(a). After compaction with sufficient shear, the composite yield surface reduces to the form illustrated in Figure 5(b).

3.4. Closing comments

This section provides the description of a basic constitutive model for a joint. The elasticity model is isotropic but nonlinear with a constant Poisson's ratio. The plasticity model includes both compaction and shear. The effects of shear-enhanced compaction and dilatation due to asperities are included. In addition, joint opening is carried as a positive value of the normal plastic strain component, and tangential motion is reflected through corresponding values of plastic shear strain.

In the next section, the structure for handling a joint in a finite element framework is given together with the outline of a numerical algorithm. Example stress–strain paths are given to illustrate the features of the joint constitutive equation by itself, and then in combination with a layer of rock.

4. CONSTITUTIVE APPROACH FOR AN ELEMENT CONTAINING A JOINT

4.1. Preliminary remarks

The finite element method is widely used so this section provides a procedure for relating joint and rock stresses and strains to corresponding stress and strain for an element. The stress, $\boldsymbol{\sigma}$, and strain, $\boldsymbol{e}$, for an element are defined with no superscript. Only cube-shaped elements of side h and with one joint parallel to one side of the element are considered. Because the eight-node brick element provides a representation for the displacement field that is complete to only first-order polynomials,

DOI: 10.1002/nag

we assume in the following that the components of strain are constant over each element as obtained, for example, by evaluating the components at the center of each element. The potential singularity in the stiffness matrix can be removed by hourglass control, a procedure that is considered to be more efficient than the alternative approach of evaluating the stress at multiple points within an element. The configuration is shown in Figure 7. The width of the rock within the element is

$$w^R = h - w^J \tag{52}$$

It is useful to define dimensionless widths for the rock and joint as follows:

$$\overline{w}^J = \frac{w^J}{h} \quad \overline{w}^R = \frac{w^R}{h} \quad \overline{w}^J + \overline{w}^R = 1 \tag{53}$$

Strains and stresses are assumed to be piece-wise constant over the respective domains defined by the joint and rock. If element strain components are prescribed, then the objective is to obtain increments for the joint and rock strains so that the deformation is compatible, equilibrium (traction) is fulfilled, and the joint and rock constitutive equations are satisfied.

4.2. Kinematic and equilibrium requirements

Suppose a strain increment, $\Delta\boldsymbol{e}$, is prescribed for the element. The objective is to find the corresponding increments in strain for the joint, $\Delta\boldsymbol{e}^J$, and the rock, $\Delta\boldsymbol{e}^R$, the stress in the joint, $\boldsymbol{\sigma}^J$, the stress in the rock, $\boldsymbol{\sigma}^R$, and finally, the stress, $\boldsymbol{\sigma}$, in the element.

4.2.1. Kinematic requirement. First, it is assumed that increments of strain $\Delta e_{tt}, \Delta e_{pp}$, and Δe_{tp} for the joint in the $\boldsymbol{t}-\boldsymbol{p}$ plane are small in comparison with the other components because of the constraint imposed by the adjacent rock. Therefore, the kinematic restriction is imposed that

$$\Delta e^J_{tt} = \Delta e^R_{tt} = \Delta e_{tt} \quad \Delta e^J_{pp} = \Delta e^R_{pp} = \Delta e_{pp} \quad \Delta e^J_{tp} = \Delta e^R_{tp} = \Delta e_{tp} \tag{54}$$

Compatibility for the other components of strain results in

$$\Delta e_{nn} = \overline{w}^J \Delta e^J_{nn} + \overline{w}^R \Delta e^R_{nn} \quad \Delta e_{nt} = \overline{w}^J \Delta e^J_{nt} + \overline{w}^R \Delta e^R_{nt} \quad \Delta e_{pn} = \overline{w}^J \Delta e^J_{pn} + \overline{w}^R \Delta e^R_{pn} \tag{55}$$

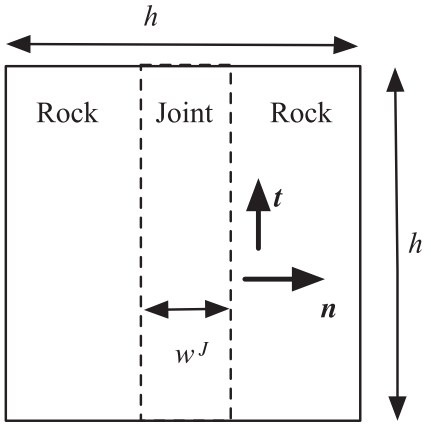

Figure 7. Notation for an element containing a joint.

DOI: 10.1002/nag

4.2.2. Equilibrium requirement. The appropriate components of stress for the element, the joint, and the rock, must satisfy traction continuity

$$\tau_n = \tau_n^J = \tau_n^R \quad \tau_t = \tau_t^J = \tau_t^R \quad \tau_p = \tau_p^J = \tau_p^R \tag{56}$$

and the remaining components satisfy overall equilibrium, as follows:

$$\sigma_{tt} = \overline{w}^J \sigma_{tt}^J + \overline{w}^R \sigma_{tt}^R \quad \sigma_{pp} = \overline{w}^J \sigma_{pp}^J + \overline{w}^R \sigma_{pp}^R \quad \sigma_{tp} = \overline{w}^J \sigma_{tp}^J + \overline{w}^R \sigma_{tp}^R \tag{57}$$

The equilibrium conditions of (56) and (57) can also be expressed in terms of increments.

4.3. Numerical procedure

For a given increment in the element strain tensor, the object is to obtain stress and strain components for the element, the joint, and the rock, with a numerical procedure that satisfies the constitutive equations, and the kinematic and equilibrium requirements.

First, note that the increments in (54) are prescribed and not altered for a step. Each of the remaining strain component increments is assigned an initial value equal to each other and to the assigned element strain increments, that is, start with

$$\Delta e_{nn}^J = \Delta e_{nn}^R = \Delta e_{nn} \quad \Delta e_{nt}^J = \Delta e_{nt}^R = \Delta e_{nt} \quad \Delta e_{np}^J = \Delta e_{np}^R = \Delta e_{np} \tag{58}$$

Note that (55) is satisfied. Perform the following update:

$$\begin{array}{ccc} e_{nn} \leftarrow e_{nn} + \Delta e_{nn} & e_{nn}^J \leftarrow e_{nn}^J + \Delta e_{nn}^J & e_{nn}^R \leftarrow e_{nn}^R + \Delta e_{nn}^R \\ e_{nt} \leftarrow e_{nt} + \Delta e_{nt} & e_{nt}^J \leftarrow e_{nt}^J + \Delta e_{nt}^J & e_{nt}^R \leftarrow e_{nt}^R + \Delta e_{nt}^R \\ e_{np} \leftarrow e_{np} + \Delta e_{np} & e_{np}^J \leftarrow e_{np}^J + \Delta e_{np}^J & e_{np}^R \leftarrow e_{np}^R + \Delta e_{np}^R \end{array} \tag{59}$$

Apply the relevant constitutive equations and update the corresponding stress component for joint and rock. Define weighted residuals of the components of traction as follows:

$$R_n = \overline{w}^J \overline{w}^R \left(\tau_n^R - \tau_n^J\right) \quad R_t = \overline{w}^J \overline{w}^R \left(\tau_t^R - \tau_t^J\right) \quad R_p = \overline{w}^J \overline{w}^R \left(\tau_p^R - \tau_p^J\right) \tag{60}$$

If the magnitudes of the residuals are sufficiently small, a traction equilibrium solution has been obtained. The reason for the coefficient $\overline{w}^J \overline{w}^R$ is that if the thickness of either the joint or the rock is 0, there is no need for equilibrium iterations. If the criteria on the residuals are not satisfied, then obtain sub-increments in strain and traction that reduce the magnitudes of the residuals. The governing equations are derived next for an iterative process similar to the Newton–Raphson procedure to force the residuals to 0.

Suppose components of strain are considered to be the primary variables. Because the total strain increments for the element are fixed, the corresponding sub-increments for the element are 0, and from (55), the sub-increments in strain for the rock, $\delta e_{nn}^R, \delta e_{nt}^R$ and δe_{np}^R, and for the joint, $\delta e_{nn}^J, \delta e_{nt}^J$ and δe_{np}^J, must satisfy

$$\overline{w}^J \delta e_{nn}^J + \overline{w}^R \delta e_{nn}^R = 0 \quad \overline{w}^J \delta e_{nt}^J + \overline{w}^R \delta e_{nt}^R = 0 \quad \overline{w}^J \delta e_{pn}^J + \overline{w}^R \delta e_{pn}^R = 0 \tag{61}$$

Because only one normal strain and two components of shear strain are involved, and under the assumption of an elastic step, the constitutive equations yield

DOI: 10.1002/nag

$$\begin{aligned} \delta\tau_n^R &= E_1^R \delta e_{nn}^R \quad & \delta\tau_n^J &= \overset{\tan}{E}{}_1^J \delta e_{nn}^J \\ \delta\tau_t^R &= 2G^R \delta e_{nt}^R \quad & \delta\tau_t^J &= 2\overset{\tan}{G}{}^J \delta e_{nt}^J \\ \delta\tau_p^R &= 2G^R \delta e_{np}^R \quad & \delta\tau_p^J &= 2\overset{\tan}{G}{}^J \delta e_{np}^J \end{aligned} \tag{62}$$

From (60) the corresponding equations for sub-increments of the residuals are

$$\delta R_n = \overline{w}^J \overline{w}^R \left(\delta\tau_n^R - \delta\tau_n^J\right) \quad \delta R_t = \overline{w}^J \overline{w}^R \left(\delta\tau_t^R - \delta\tau_t^J\right) \quad \delta R_p = \overline{w}^J \overline{w}^R \left(\delta\tau_p^R - \delta\tau_p^J\right) \tag{63}$$

Choose these sub-increments to satisfy

$$\delta R_n = -R_n \quad \delta R_t = -R_t \quad \delta R_p = -R_p \tag{64}$$

Define weighted elastic moduli as follows:

$$E^{RJ} = \overline{w}^R \overset{\tan}{E}{}_1^J + \overline{w}^J E_1^R \quad \mathrm{G}^{RJ} = \overline{w}^R \overset{\tan}{G}{}^J + \overline{w}^J G^R \tag{65}$$

Then the use of (63), (64), and (61) yields specific equations for sub-increments in strain for both joint and rock:

$$\begin{aligned} \delta e_{nn}^J &= \frac{R_n}{E^{RJ}\overline{w}^J} \quad & \delta e_{nt}^J &= \frac{R_t}{2G^{RJ}\overline{w}^J} \quad & \delta e_{np}^J &= \frac{R_p}{2G^{RJ}\overline{w}^J} \\ \delta e_{nn}^R &= -\frac{R_n}{E^{RJ}\overline{w}^R} \quad & \delta e_{nt}^R &= -\frac{R_t}{2G^{RJ}\overline{w}^R} \quad & \delta e_{np}^R &= -\frac{R_p}{2G^{RJ}\overline{w}^R} \end{aligned} \tag{66}$$

These strain increments are sent to the respective constitutive equations for rock and joint. In the rock constitutive subroutine, the increments in traction will be identical to those given in (62). In the joint constitutive equation, the total strain sub-increments will consist of elastic and plastic parts, so the resulting sub-increments in traction will differ from those given in (62), and an iterative correction is necessary. The constitutive equation algorithms provide the updates for all stress and elastic and plastic strain components.

In summary, the iterative procedure for forcing traction equilibrium consists of the following:

Start of Equilibrium Algorithm

1. Begin by assuming strain increments in joint and rock equal increments in element from (54) and (58). Apply constitutive equation algorithms for rock and joint to obtain components of traction.
2. Determine the weighted residual of (60). If the magnitudes of the residuals are less than the given criteria, equilibrium has been obtained and the procedure is stopped. Otherwise proceed to the next step.
3. Compute sub-increments in joint and rock strain using (66).
4. Call the constitutive equations for rock and strain to obtain sub-increments in traction.
5. Update tractions and go to Step 2.

End of Equilibrium Algorithm

4.3.1. Handling a gap. There is a possibility that a gap may initiate based on a positive value of either τ_n^R or τ_n^J after the use of the trial elastic step of (54) and (58). Now, the traction equilibrium conditions are replaced with the conditions that the traction components are 0. First, consider the normal component. Sub-increments $\left(\delta e_{nn}^R, \delta e_{nn}^{J,e}, \delta e_{nn}^{J,p}\right)$ are considered that force both τ_n^R and τ_n^J to 0, or

DOI: 10.1002/nag

$$\delta e_{nn}^{R} = -\frac{\tau_n^R}{E_1^R} \quad \delta e_{nn}^{J,e} = -\frac{\tau_n^J}{E_1^J} \tag{67}$$

in which $\overset{\tan}{E}{}_1^J$ is replaced with $E_{1,0}^J$, because if the traction is 0, the volumetric elastic strain will be small. The first of (61) becomes

$$\overline{w}^J\left(\delta e_{nn}^{J,e} + \delta e_{nn}^{J,p}\right) + \overline{w}^R \delta e_{nn}^R = 0 \tag{68}$$

from which the sub-increment in plastic strain is

$$\delta e_{nn}^{J,p} = R_G \quad R_G \equiv -\frac{1}{\overline{w}^J}\left(\overline{w}^J \delta e_{nn}^{J,e} + \overline{w}^R \delta e_{nn}^R\right) \tag{69}$$

The requirement for gap initiation or gap opening is that $R_G > 0$.

However, there is also the possibility that a gap already exists as indicated by a positive value of $e_{nn}^{J,p}$. The current step may make the gap larger or may reduce the gap width if $\delta e_{nn}^{J,p} < 0$. The result is that (69) is applied if either $R_G > 0$ or $e_{nn}^{J,p} > 0$.

Once a gap is formed, the shear traction components must be reduced to 0, and the corresponding plastic components of strain adjusted to account for the tangential slip. The adjustments in elastic strain components and traction are the following:

$$\begin{aligned} &\delta e_{nt}^R = -\frac{\tau_t^R}{G^R} && \delta e_{nt}^{J,e} = -\tau_t^J \overset{\tan}{G}{}^J \\ &\delta e_{pn}^R = -\frac{\tau_p^R}{G^R} && \delta e_{pn}^{J,e} = -\tau_p^J \overset{\tan}{G}{}^J \\ &\tau_t^R = 0 \quad \tau_p^R = 0 && \tau_t^J = 0 \quad \tau_t^J = 0 \end{aligned} \tag{70}$$

In analogy with (69), the sub-increments in shear components of plastic strain are

$$\begin{aligned} \delta e_{nt}^{J,p} &= -\frac{1}{\overline{w}^J}\left(\overline{w}^J \delta e_{nt}^{J,e} + \overline{w}^R \delta e_{nt}^R\right) \\ \delta e_{pn}^{J,p} &= -\frac{1}{\overline{w}^J}\left(\overline{w}^J \delta e_{pn}^{J,e} + \overline{w}^R \delta e_{pn}^R\right) \end{aligned} \tag{71}$$

By placing the formation of a gap within a constitutive equation formulation, there is no need for a separate contact-impact algorithm.

4.4. Closing comments

In this section, an isotropic elastic constitutive equation is used to model rock and an elastic-plastic model is used for the joint. Because the joint width is a constitutive variable, the same constitutive equation can be used for faults, which are typically defined by much larger widths. The joint constitutive equation involves nonlinear elasticity with a constant Poisson's ratio and a plasticity model consisting of three parts to account for compaction, shear, and zero traction. For each part, a yield function and evolution equations are prescribed so that a conventional plasticity algorithm can be used.

The kinematic and equilibrium equations used to account for an element that consists of a joint included within rock are also described. These equations are solved numerically rather than analytically, although an analytical solution could provide a more efficient numerical algorithm. However, by using the proposed numerical approach, the constitutive equations for rock and joint

DOI: 10.1002/nag

are treated separately, with the implication that if either constitutive equation is modified to accommodate agreement with experimental data, the overall structure remains unchanged.

5. FEATURES OF THE JOINT CONSTITUTIVE MODEL

5.1. Values for material parameters and dimensionless variables

Because the joint is considered embedded within a rock, values of constitutive parameters for rock are considered first. Granite is chosen for illustrative purposes. Within the wide range of values suitable for granite, the following values have been chosen:

$$\begin{aligned} Y^R &= 60\,GPa \qquad \nu^R = 0.2 \qquad \rho^R = 2,600 kg/m^3 \\ f_C^R &= 240 MPa \quad \tau_{nf}^R = 24 MPa \end{aligned} \tag{72}$$

in which ρ^R, f_C^R, and τ_{nf}^R denote mass density, compressive failure stress, and tensile failure stress, respectively. With these choices, it follows that

$$E_1^R = 66\ \ GPa \quad E_2^R = E_1^R/4 \quad 2G^R = 50\ \ GPa \tag{73}$$

and the speed of wave propagation for uniaxial strain is

$$c_{stn}^R = \left(E_1^R/\rho^R\right)^{1/2} = 5,000\ \ m/s \tag{74}$$

Dimensionless variables, denoted with a bar, are chosen next. Let σ_{ref} and E_{ref} denote reference values for stress and elasticity, respectively. Although strain is already dimensionless, it is convenient to scale strain with a reference strain, e_{ref}. Then dimensionless variables become

$$\overline{\boldsymbol{\sigma}}^R = \frac{\boldsymbol{\sigma}^R}{\sigma_{ref}} \quad \overline{\boldsymbol{e}}^R = \frac{\boldsymbol{e}^R}{e_{ref}} \quad \overline{E}_1^R = \frac{E_1^R}{E_{ref}} \quad \overline{E}_2^R = \frac{E_2^R}{E_{ref}} \quad \overline{G}^R = \frac{G^R}{E_{ref}} \tag{75}$$

Poisson's ratio is already dimensionless.

It is assumed that for the problems under consideration, any component of normal stress is less than the compresive failure stress, so f_C^R is chosen as the reference stress σ_{ref} . Choose a reference elastic modulus to be $E_{ref} = E_1^R$. For convenience, choose the reference strain to be

$$e_{ref} = f_c^R/E_1^R = 0.004 \tag{76}$$

Then the constitutive equations, illustrated with one normal component and one shear component, become

$$\overline{\sigma}_{nn}^R = \overline{E}_1^R \overline{e}_{nn}^R + \overline{E}_2^R\left(\overline{e}_{tt}^R + \overline{e}_{pp}^R\right) \quad \overline{\sigma}_{nt}^R = 2\overline{G}^R \overline{e}_{nt}^R \tag{77}$$

in which

$$\overline{E}_1^R = 1 \quad \overline{E}_2^R = \frac{\nu^R}{1-\nu^R} = 0.25 \quad 2\overline{G}^R = \frac{(1-2\nu^R)}{(1-\nu^R)} = 0.75 \quad \nu^R = 0.2 \tag{78}$$

The range of absolute values of components of stress and strain will be [0, 1].

DOI: 10.1002/nag

5.2. Dimensionless variables and material parameters for a joint

First, assume that stress, strain, and the elastic tangent parameters in the joint have been scaled by the same parameters used for rock. The parameters used in the elastic part of the joint constitutive equation are E_M^J, E_0^J, v_0^J, $e_{ref}^{J,e}$, and m^e so their dimensionless counterparts are

$$\overline{E}_M^J = \overline{E}_1^R = 1 \quad \overline{E}_0^J = \frac{E_0^J}{E_1^R} \quad \overline{e}_{ref}^{J,e} = \frac{e_{ref}^{J,e}}{e_{ref}} \tag{79}$$

and v_0^J and m^e are already dimensionless. The initial value of the tangent stiffness must satisfy $0 < \overline{E}_0^J \leq 1$. The dimensionless reference elastic strain $\overline{e}_{ref}^{J,e}$ may be larger than unity. For example, if $\overline{e}_{ref}^{J,e} = 3$, then the elastic volumetric strain at which the elasticity part becomes linear is $e_{ref}^{J,e} = 0.012$.

Similarly, for the plasticity part, all traction components and yield functions are divided by f_c^R to obtain dimensionless variables. All strain components and strain parameters are scaled by e_{ref}. For the compaction part, the dimensionless material parameters become $m^p, \overline{e}_0^{J,p} = e_0^{J,p}/e_{ref}$ and $\overline{E}_0^{J,p} = \overline{E}_0^{J,p}/E_{ref}$, and for the shear part the corresponding parameters are $\overline{e}_{a0}^{J,p} = e_{a0}^{J,p}/e_{ref}, \overline{\tau}_{a0}^J = \tau_{a0}^J/f_c^R$ and μ^J.

5.3. Element variables

With the assumption that dimensionless constitutive variables, including element stress and strain components, are used consistently, the overbars are dropped. Increments of components of element strain, $\Delta \boldsymbol{e}$, are prescribed for the element constitutive equation subroutine, and the element stress, $\boldsymbol{\sigma}$, is obtained. The value of the element size, h, does not explicitly appear in the constitutive equations; only indirectly through the definitions of the relative widths of the joint and rock, $\overline{w}^J$ and $\overline{w}^R$, respectively. Values for the following constitutive and element variables must be prescribed: rock elasticity parameters: E_1^R, v^R; joint elasticity parameters: E_M^J, E_0^J, v_0^J, $e_{ref}^{J,e}$, m^e; and joint plasticity parameters: $E_0^{J,p}, m^p$, $e_0^{J,p}$, μ^J, τ_{a0}^J $e_{a0}^{J,p}$.

Recall that all the strain components for the rock, and the strain components, $e_{tt}^J, e_{pp}^J, e_{tp}^J$, for the joint are elastic only. Furthermore, $e_{tt}^J = e_{tt}^R = e_{tt}$, $e_{pp}^J = e_{pp}^R = e_{pp}$, and $e_{tp}^J = e_{tp}^R = e_{tp}$ so these joint and rock variables do not have to be saved separately. The nonlinear joint elasticity model requires the volumetric elastic strain that is available as the sum of the normal strains. The joint plasticity model uses the normal component of plasticity as a parameter.

Therefore, there is a total of 22 internal variables that must be stored as part of the element constitutive equation subroutine. They are the following:

a. the six components of joint stress, $\sigma_{nn}^J, \sigma_{nt}^J, \sigma_{np}^J, \sigma_{tt}^J, \sigma_{pp}^J, \sigma_{tp}^J$,
b. the six components of rock stress, $\sigma_{nn}^R, \sigma_{nt}^R, \sigma_{np}^R, \sigma_{tt}^R, \sigma_{pp}^R, \sigma_{tp}^R$,
c. nine components of strain consisting of the rock strains, $e_{nn}^R, e_{nt}^R, e_{np}^R$, the elastic joint strains, $e_{nn}^{J,e}, e_{nt}^{J,e}, e_{np}^{J,e}$, and the plastic joint strains, $e_{nn}^{J,p}, e_{nt}^{J,p}, e_{np}^{J,p}$, and
d. one plastic shear history variable, $\widehat{e}_s^{J,p}$.

The relatively large number of history variables is the price paid to maintain the flexibility of being able to change either the joint or the rock constitutive equation without doing the algebra so that equilibrium and kinematic equations within the element are automatically satisfied.

5.4. Representative features of the joint constitutive model

5.4.1. Values of material parameters. First, we provide a brief summary of the effects of changes in values of the material parameters on the predicted stress–strain response of a joint for simple paths. Later, the features of the model are shown for more complicated paths that include combined compaction and shear, the creation of gaps, handling an initial gap, and the combination of joint and rock within an element.

DOI: 10.1002/nag

Certain material parameters are self explanatory and are not varied. These parameters are the uniaxial strain, elastic parameter for rock, Poisson's ratio for rock, the cohesive strength of the joint under zero normal stress, and the Mohr–Coulomb friction parameter for the joint. The fixed values chosen for these parameters are

$$E_1^R = 1 \quad \nu^R = 0.2 \quad \tau_{a0}^J = 0.1 \quad \mu^J = 0.4 \tag{80}$$

The values assigned for the other material parameters for each figure are given in Table I. The entry 'Varies' implies that the various values for this parameter are provided within the figure. The choice of $\overline{W}^J = 1$ provides an element that is composed entirely of joint material. A smaller value of $\overline{W}^J$ implies that the constitutive element response includes both joint and rock.

5.4.2. Compaction. The first set of results are designed to indicate the effects of material parameters on predictions of uniaxial strain compaction. Because the components of plastic normal strain in the t- and p-directions are 0, the normal components of elastic and plastic strains, $e_{nn}^{J,e}$ and $e_{nn}^{J,p}$, respectively, are equal to the corresponding elastic and plastic volumetric strains.

The plots shown in Figure 8(a) show that for a given value of stress, reductions in the value of the initial elastic modulus, E_0^J, result in an increase in elastic strain. A corresponding result holds for plastic strain as a function of the initial plastic modulus, $E_0^{J,p}$, as shown in Figure 8(b). As shown in Figure 8(c) an increase in the exponent, m^e, provides an increase in elastic strain. The value $m^e = 1$ provides a linear relation, and $m^e < 1$ would yield a relation more suitable for rubber, at least for small strains. The plot of Figure 8(d) indicates an inverse relation between the exponent m^p and the plastic strain. The results of Figure 8(e) and (f) suggest that changes in values of the reference elastic strain, $e_{ref}^{J,e}$, and the reference plastic strain, $e_{ref}^{J,p}$, provide the largest changes in predicted elastic and plastic strain, respectively. These are probably the most important parameters for fitting experimental data.

5.4.3. Combined compaction and shear. Next, we provide a brief summary of the predicted response of the joint under combined compaction and shear. The effects of values for the slope of the shear part of the yield surface, μ^J, and the initial strength in shear due to asperities, τ_{a0}^J, are self-evident. We show the effects of the two remaining parameters, the normal compaction and the accumulated shear strain, $e_{a0}^{J,p}$, on the shear response. We illustrate shear behavior by first loading in compaction under uniaxial strain, and then superimposing a shear strain while holding the compaction strain fixed. The loading part of the shear response is strictly elastic until the limit surface is reached. Then shear softening occurs accompanied by dilatation, which causes the compaction surface to soften as well. The compaction part of the yield surface is then activated. The normal stress causes strain hardening. The overall effect for this path is that the compaction surface remains stationary in stress space during the shear-loading phase.

Table I. Values of material parameters used for plots shown in specified figures.

Figure\Parameter	$\overline{W}_J$	E_0^J	m^e	$e_{ref}^{J,e}$	$E_0^{J,p}$	m^p	$e_{ref}^{J,p}$	$e_{a0}^{J,p}$
8(a)	1	Varies	2	−1.5	0.2	2	−1.5	1.6
8(b)	1	0.2	2	−1.5	Varies	2	−1.5	1.6
8(c)	1	0.2	Varies	−1.5	0.2	2	−1.5	1.6
8(d)	1	0.2	2	−1.5	0.2	Varies	−1.5	1.6
8(e)	1	0.2	2	Varies	0.2	2	−1.5	1.6
8(f)	1	0.2	2	−1.5	0.2	2	Varies	1.6
9(a)	1	0.2	2	−1.5	0.2	2	−1.5	1.6
9(b)	1	0.2	2	−1.5	0.2	2	−1.5	Varies
10	1	0.1	4	−3.0	0.1	4	−3.0	1.6
11	1	0.2	2	−1.5	0.2	2	−1.5	1.6
12	Varies	0.1	4	−3.0	0.1	4	−3.0	1.6
13	Varies	0.2	2	−1.5	0.2	2	−1.5	1.6

DOI: 10.1002/nag

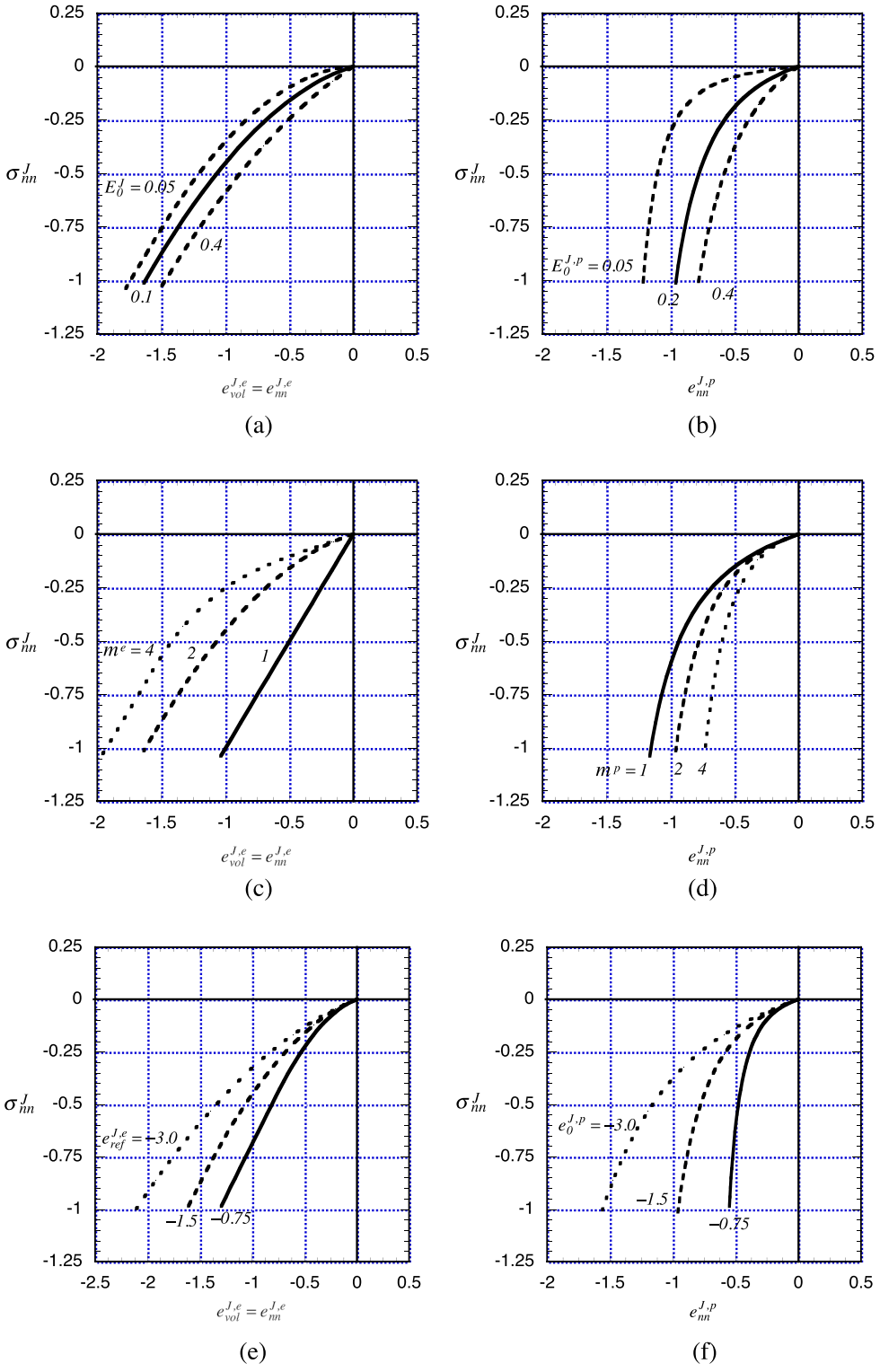

Figure 8. The effects of changes from standard values of particular material parameters on plots of stress versus strain for loading in uniaxial strain. (a) Effect of E^J_0. (b) Effect of $E^{J,p}_0$. (c) Effect of m^e. (d) Effect of m^p. (e) Effect of $e^{J,e}_{ref}$. (f) Effect of $e^{J,p}_{ref}$.

Figure 9(a) shows the shear stress–strain response for three values of the normal compaction stress σ^J_{nn}. Because of the rather elementary yield surface for shear, the response is elastic up to the initial

DOI: 10.1002/nag

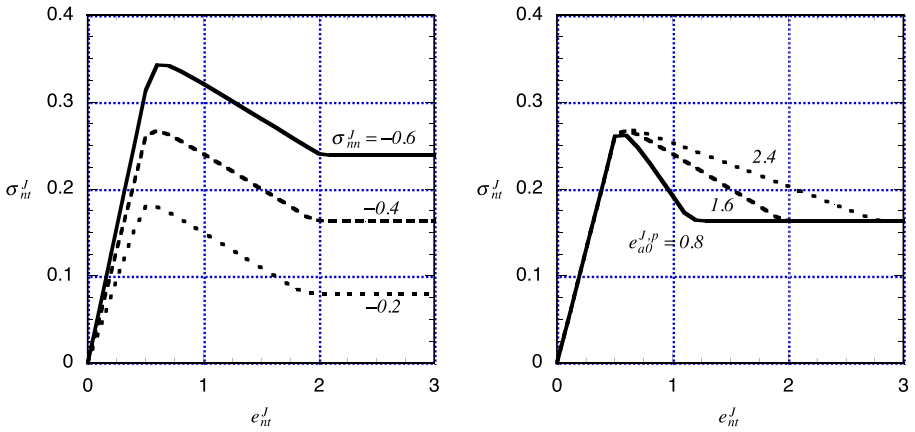

Figure 9. Response of joint in shear showing effects of normal stress and the shear strain parameter. (a) Effect of normal stress, σ^J_{nn}. (b) Effect of asperity shear term, $e^{J,p}_{a0}$.

yield stress. The nonlinear elastic aspect of the model is reflected through the different slopes for the elastic loading segments. After the yield surface is activated, the response is one of softening until the residual Mohr–Coulomb surface is reached. Next, for the choice of $\sigma^J_{nn} = -0.4$, we illustrate the expected variation of softening slope reflected by different values for $e^{J,p}_{a0}$ in Figure 9(b).

To reflect experimental data for shear when compaction is followed by shear loading, an alternative form must be used for the shear yield function. The yield surface should evolve to a limit surface similarly to the initial yield surface in this work, and then soften. Moreover, as suggested by Barton [25], the limit surface itself should have a limiting value of maximum shear stress for large negative values of σ^J_{nn} (or for large mean pressure).

As illustrated in Figure 10(a), we consider a slightly more complicated path in strain space, to indicate the features that are implicit with the model. First, the material is loaded in uniaxial strain compression as indicated by segment O-A. Then negative increments of uniaxial strain are prescribed simultaneously with positive increments in shear strain to obtain segment A-F. Intermediate letters identify points of significance with regard to the elasto-plastic response. A corresponding plot of shear stress versus normal stress is given in Figure 10(b), of normal stress versus normal plastic strain in Figure 10(c), and of shear stress versus plastic shear in Figure 10(d).

For segment A-B, the response is elastic so the plastic components do not change until the stress reaches the initial yield surface for shear at point B. Then softening causes the shear stress to reduce with plastic volumetric dilatation, or positive increments in plastic normal strain. Dilatation is shown in segment B-C-D in Figure 10(c) as a reduction in the normal component of plastic strain. This reduction comes to an end once the maximum amount of shear softening is reached at point D. As indicated by (43), no additional dilatation is allowed to accumulate once the effective plastic strain $e^{J,p}_s$ attains the value $e^{J,p}_{a0}$. For segment B-C, the increments in total normal strain are positive but with a smaller magnitude than those of the plastic strain increments. The result is that the elastic strain increments are negative so the negative normal stress increases in magnitude as indicated in Figure 10(b). After point C, the amount of dilatation is reduced to the point that the normal elastic strain increments become positive and the normal component of stress resumes the expected property of reducing in magnitude. At point D, the initial yield surface has softened to the Mohr–Coulomb surface. For the subsequent leg, D-E, the shear response is one of perfect plasticity, while the normal part is elastic with no change in normal plastic strain. At point E, both the shear and normal components of stress have reduced to 0. The continuation of the path in segment E-F results in a reduction of the normal plastic strain, as shown in Figure 10(c), and represents an opening of the joint, that is, the formation of a gap. Similarly, Figure 10(d) shows a continued increase in the shear plastic strain to a final value of approximately 4.4. This value is greater than the total shear

DOI: 10.1002/nag

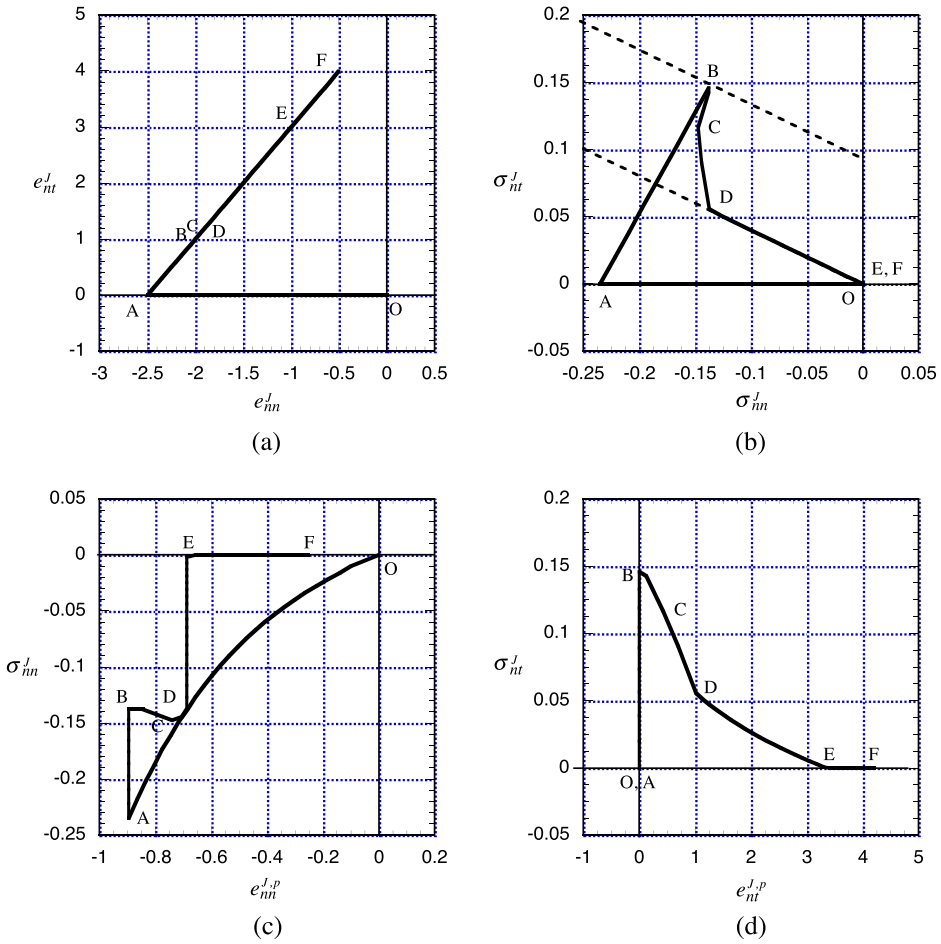

Figure 10. A path showing the interaction of compaction and shear. (a) Path in strain space. (b) Path in stress space. (c) Normal stress versus normal plastic strain. (d) Shear stress versus shear plastic strain.

strain of value 4 shown in Figure 10(a) and is a consequence of the elementary form for nonlinear elasticity where the shear modulus is highest for the loading phase A-B, and then is of a reduced value for segment D-E. As these plots show, the interaction of elasticity and plasticity, and or shear and normal effects, can be quite intricate, and care must be taken in interpreting the response provided by a model. However, these rather elementary examples provide a basis for examining the behavior of more complicated, and presumably more realistic, models that include shear-enhanced compaction and improved interaction predictions involving shear and normal stress components.

5.4.4. Compaction and unloading of the joint with gap formation. This example is one of uniaxial strain designed to show the general features of a joint associated with compression, unloading, gap formation and closure, and reloading. In Figure 11, plots of normal stress versus plastic strain, elastic strain and total strain illustrate the features of the plasticity, elasticity, and total element response of the joint constitutive equation. The initial loading phase O-A shows simultaneously the nonlinear features of both the elasticity and the hardening part of plasticity during loading. Upon unloading for segment A-B, the elasticity path is re-traced while the plastic strain remains fixed. Additional positive increments of strain provide segment B-D where the total strain equals the plastic strain. Further positive increments in total strain provide segment D-C and represents the formation of a gap. Again, the total strain equals the plastic strain and the gap width equals the joint width times the plastic strain. Negative increments in total strain provide segment C-D and represents gap closure. Finally, further negative increments for total strain provide segment D-E that

DOI: 10.1002/nag

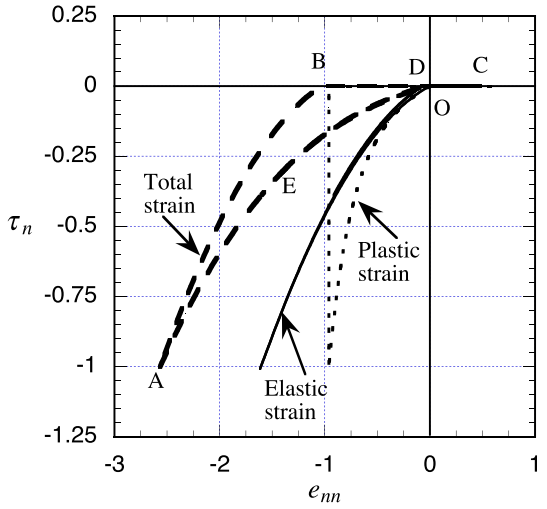

Figure 11. Traction versus uniaxial strain for compaction, unloading, gap formation and reloading.

corresponds to reloading the material. The model does not contain a kinematic hardening feature so that reloading from zero strain follows the initial loading curve.

5.4.5. Pre-existing gap. Occasionally, the experimentally determined relationship between normal stress and normal strain shows an initial loading phase where the stress remains approximately zero as the strain increases. A simple approach to handling this phase is to treat it as a gap. To this end, assume the stress is actually zero in this phase and assign an initial value of plastic normal strain equal to the strain associated with this initial loading. Then the stress becomes nonzero only after the gap closes.

5.4.6. Element response for variable joint widths. Figure 12 shows the effect of the dimensionless width of the joint on the stress–strain response of the element. In each case, compressive strain increments are prescribed until the normal stress equals -1. The plots of stress versus joint elastic strain and plastic strain are identical for all values of $\overline{W}^J$ as is the plot of stress versus rock strain. The only part that changes is stress versus element strain as shown for the cases where the joint width equals h, h/2, h/4, and h/8 or $\overline{W}^J = 1, 1/2, 1/4$ and 1/8, respectively. As expected, when the

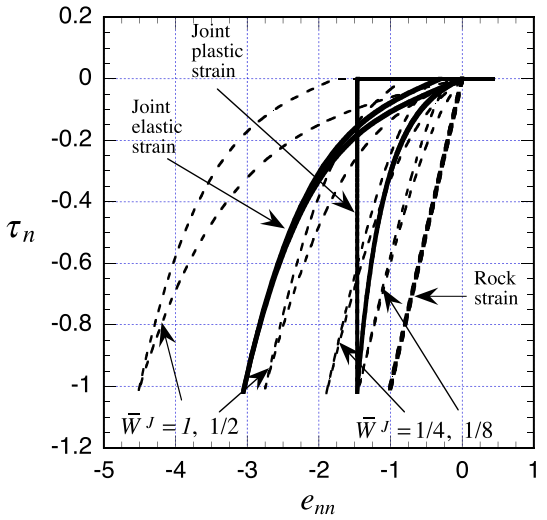

Figure 12. Normal stress versus strain for loading, unloading, and extension to positive strain showing the effects of variable joint width.

DOI: 10.1002/nag

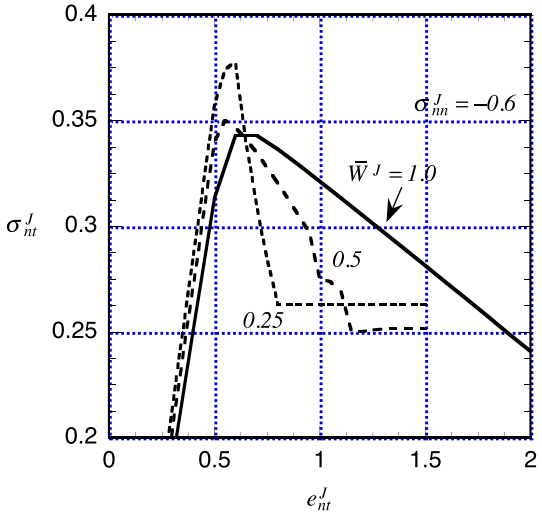

Figure 13. Shear stress softening with different joint sizes.

width of the joint is decreased, the response of the element transitions from the response of the joint to a response that is closer to that of the rock.

5.4.7. Element softening. Next, in Figure 13, element shear stress versus element shear strain is shown for the path described previously in Figure 9 but with various ratios of joint width to element width. Note that the peak shear stress and the final Mohr–Coulomb residual values vary with the relative joint width because the plastic joint normal strain for a given normal compaction stress varies with the relative joint width. Part of the normal strain in the element is associated with rock. The key feature of this plot is that the softening portions of the stress–strain curves become steeper as the width of the joint becomes smaller relative to the width of rock in an element. Ultimately, a stress reversal will appear and conventional numerical algorithms will not work. The suggested approach is to monitor the situation for a given choice of material parameters and choose an element size so that stress reversal, or even abrupt softening, does not occur.

5.5. Concluding remarks

This section illustrates that the proposed joint model provides the following features: (i) nonlinear elasticity; (ii) elastic-plastic compaction; (iii) dilatation under initial shear; (iv) no additional dilatation after a certain amount of shear (Mohr–Coulomb); (v) gap formation; (vi) gap closure and reloading with no hysteresis; (vii) treatment of initial gaps; and (viii) satisfaction of kinematic and equilibrium constraints within an element for a joint aligned with an element side.

6. SUMMARY AND CONCLUSIONS

We have described a basic joint constitutive model with a composite yield surface composed from three individual surfaces that separately govern joint behavior in compaction, shear, and tension. The composite surface is constructed to reflect the following combined features:

i. The tensile strength is 0.
ii. Gap formation and sliding are tracked through normal and shear components of plastic strain.
iii. Compaction is governed by nonlinear elasticity with plasticity.
iv. Shear under compressive or zero normal traction is nonlinearly elastic up to a limit state followed by non-associative softening with dilatation to a residual Mohr–Coulomb plasticity with no further dilatation.
v. The dilatation from shear softens the compaction yield surface, as does gap formation.

DOI: 10.1002/nag

vi. These characteristic features were illustrated by computing the predicted constitutive response for a variety of prescribed stress and strain paths. A parameter study was also performed to delineate the inherent variability in the model and also to indicate the model's versatility and adaptability to fit experimental data.

The multi-surface construction of the yield surface provides a general framework for constructing yield surfaces that can accommodate more complicated joint constitutive behavior. The emphasis in this work has been on the description of joint behavior under compaction with a relatively simple model for shear. For example, a different form for the yield function could be used to reflect an inelastic response under shear up to the limit surface. Other authors have addressed this aspect of joint behavior in considerable detail, and there is no reason why these more detailed yield surfaces could not be included within the current framework.

A fairly standard Newton–Raphson procedure is used to determine the elastic-plastic behavior of joints as governed by the constitutive model. An additional, Newton–Raphson procedure is introduced to impose equilibrium constraints when a joint is embedded in rock and the joint is not resolved by the finite element discretization. The numerical technique allows a joint and rock to exist within a single finite element with the effective behavior fully described. The joint can be of arbitrary width within the element, but is so far limited to be parallel to the side of a square element. It is also possible to have a joint span more than one element, as might be sensible for a simulation involving a fault. Moreover, the model can describe multiple joints within an element if they are represented as a single joint with an effective width. This formulation is analogous to defining a representative volume element and using a continuum representation of joints for large-scale simulations. The advantage here is that the detailed properties of the joint are automatically included within the formulation.

Our main objectives have been: (i) to show that the essential features of joint behavior can be captured with a rather elementary constitutive equation; (ii) to argue that gap formation and sliding can be captured within the constitutive equation; (iii) to provide the joint width as a primary variable so that sliding and gaps are handled within the constitutive equation; and (iv) to describe a numerical algorithm for handling joints of arbitrary width within an element. We believe these are significant items not readily available in the technical literature. Ultimately, such a constitutive approach can be used to perform two-dimensional and three-dimensional studies to evaluate the relative importance of various features inherently associated with joints, and to study stress distributions in jointed rock to assess the vulnerability of important engineering structures.

ACKNOWLEDGEMENTS

This work was partially supported by Task Order #26 under Defense Threat Reduction Agency contract 01-03-D-0009 with the University of New Mexico. Initial work on the formulation by Tyler Baker and valuable comments on an initial draft by Ling Xu are greatly appreciated.

REFERENCES

1. Cook NGW. Natural joints in rock: mechanical, hydraulic and seismic behavior and properties under normal stress (Jaeger memorial dedication lecture). *International Journal Rock Mechanics and Mining Sciences & Geomechanics Abstracts* 1992; **29**(3):198–223.
2. Jing L. A review of techniques, advances and outstanding issues in numerical modelling for rock mechanics and rock engineering. *International Journal of Rock Mechanics and Mining Sciences* 2003; **40**:283–353.
3. Murakami H, Impelluso T, Hegemier GA. A continuum finite-element for single-set jointed media. *International Journal for Numerical Methods in Engineering* 1991; **31**(6):1169–1194.
4. Cai M, Horii H. A constitutive model of highly jointed masses. *Mechanics of Materials* 1992; **13**:217–246.
5. Lee U. A theory of smeared continuum damage mechanics. *Korean Society of Mechanical Engineers International Journal* 1998; **12**(2):233–243.
6. Chalhoub M, Pouya A. Numerical homogenization of a fractured rock mass: a geometrical approach to determine the mechanical representative elementaty volume. *Electronic Journal of Geotechnical Engineering* 2008; **13**(K):1–12.
7. Brannon RM, Fossum AF, Strack OE. A computational model for materials containing arbitrary joint sets. *Report prepared for the Ground Shock in Faulted Media Workshop (GSFM)*, SAIC Conference Center, McLean, VA, January 11-15, 2010; 1–44, SAND2010-2077P.

DOI: 10.1002/nag

8. Huang X, Haimson BC, Plesha ME, Oiu X. An investigation of the mechanics of rock joints – Part I: laboratory investigation. *International Journal of Rock Mechanics and Mining Science and Geomechanics Abstracts* 1993; **30**(3):257–269.
9. Asadollahi P, Invernizzi MCA, Addotto S, Tonon F. Experimental validation of modified Barton's model for rock fractures. *Rock Mechanics and Rock Engineering* 2010; **43**:597–613.
10. Plesha ME. Constitutive models for rock discontinuities with dilatancy and surface degredation. *International Journal for Numerical and Analytical Methods in Geomechanics* 1987; **11**:345–362.
11. Qiu X, Plesha ME, Huang X, Haimson BC. An investigation of the mechanics of rock joints – Part II: analytical investigation. *International Journal of Rock Mechanics and Mining Science and Geomechanics Abstracts* 1993; **30**(3):271–287.
12. Trivedi A. Strength and dilatancy of jointed rock with granular fill. *Acta Geotechnica* 2010; **5**:15–31.
13. Gens A, Carol I, Alonso EE. A constitutive model for rock joints formulation and numerical implementation. *Computers and Geotechnics* 1990; **9**:3–20.
14. Haberfield CM, Johnston IW. Mechanistically-based model for rough rock joints. *International Journal Rock Mechanics and Mining Sciences & Geomechanics Abstracts* 1994; **31**(4):279–292.
15. Huang TH, Chang CS, Chao CY. Experimental and mathematical modeling for fracture of rock joint with regular asperities. *Journal of Engineering Fracture Mechanics* 2002; **69**:1977–1996.
16. Seidel JP, Haberfield CM. A theoretical model for rock joints subjected to constant normal stiffness direct shear. *International Journal of Rock Mechanics and Mining Sciences* 2002; **39**:539–553.
17. Grasselli G, Egger P. Constitutive law for the shear strength of rock joints based on three-dimensional parameters. *International Journal of Rock Mechanics and Mining Sciences* 2003; **40**:25–40.
18. Mihai IC, Jefferson AD. A multi-asperity plastic contact crack plane model for geomaterials. *International Journal for Numerical and Analytical Methods in Geomechanics* 2012; **37**:1492–1509.
19. Bandis SC, Lumsden AC, Barton NR. Fundamentals of rock joint deformation. *International Journal of Rock Mechanics and Mining Science and Geomechanics Abstracts* 1983; **20**(6):249–268.
20. Desai CS, Fishman KL. Plasticity-based constitutive model with associated testing for joints. *International Journal of Rock Mechanics and Mining Science and Geomechanics Abstracts* 1991; **28**(1):15–26.
21. Saeb S, Amadei B. Modeling rock joints under shear and normal loading. *International Journal of Rock Mechanics and Science and Geomechanics Abstracts* 1992; **29**:267–278.
22. Wang JG, Ichikawa Y, Leung CF. A constitutive model for rock interfaces and joints. *International Journal of Rock Mechanics and Mining Sciences* 2003; **40**:41–53.
23. Schwer LE, Lindberg HE. A finite element sideline approach for calculating tunnel response in jointed rock. *International Journal for Numerical and Analytical Methods in Geomechanics* 1992; **16**:529–540.
24. Goodman RE. Introduction to rock mechanics. John Wiley, 2nd edition. 1989.
25. Barton N. Shear strength criteria for rock, rock joints, rockfill and rock masses: problems and some solutions. *Journal of Rock Mechanics and Geotechnical Engineering* 2013; **5**:249–261.

DOI: 10.1002/nag